Structural Engineering and Mechanics, *Vol. 64, No. 3 (2017) 361-379*
DOI: https://doi.org/10.12989/sem.2017.64.3.361

Vibration analysis of double-bonded sandwich microplates with nanocomposite facesheets reinforced by symmetric and un-symmetric distributions of nanotubes under multi physical fields

Mehdi Mohammadimehr*, Hassan BabaAkbar Zarei, Ali Parakandeh and Ali Ghorbanpour Arani

Department of Solid Mechanics, Faculty of Mechanical Engineering, University of Kashan, P.O. Box: 87317-53153, Kashan, Iran

(Received February 13, 2017, Revised August 11, 2017, Accepted August 18, 2017)

Abstract. In this article, the vibration behavior of double-bonded sandwich microplates with homogeneous core and nanocomposite facesheets reinforced by carbon nanotube and boron nitride nanotube under multi physical fields such as 2D magnetic and electric fields is investigated. Symmetric and un-symmetric distributions of nanotubes are considered for facesheets of sandwich microplates such as uniform distribution and various functionally graded distributions. The double-bonded sandwich microplates rest on visco-Pasternak foundation. Material properties of sandwich microplates are obtained by the extended rule of mixture. The sinusoidal shear deformation theory (SSDT) is employed to describe displacement fields of sandwich microplates. Also, the dimensionless natural frequency is obtained by classical plate theory (CPT) and compared with the obtained results by SSDT. It can be seen that the obtained dimensionless natural frequencies by CPT are higher than SSDT. In order to study the material length scale parameters, modified strain gradient theory at micro scale is utilized and then, the equations of motion are derived using Hamilton's principle. The effects of different parameters such as foundation parameters including Winkler, shear layer and damping coefficients, various distributions and volume fraction of nanotubes, core to facesheet thickness ratio, aspect and side ratios on the dimensionless natural frequencies are discussed in details. The results of present work can be used to optimum design and control of similar systems such as micro-electro-mechanical and nano-electro-mechanical devices.

Keywords: vibration analysis; double-bonded sandwich microplates; nanocomposite facesheets; symmetric and un-symmetric distributions of nanotubes; 2D magnetic and electric fields

1. Introduction

Nowadays, the use of sandwich structures in many applications of engineering are developed such as transport, aerospace, marine, civil construction, and shipbuilding. It is due to the significant features of sandwich structures including high strength and stiffness with admissible flexibility, low weight and suitable durability. Thus, understanding the behavior of these structures in different conditions is very important. Moreover, the sandwich structures have been attracted by many researchers about bending, buckling and vibration behaviors.

Nayak *et al*. (2002) studied free vibration analysis of composite sandwich Reddy's plate. They showed the applicability of the Reddy type elements for a wide range of free vibration problems, with various material properties, geometric features, and boundary conditions. Wang *et al*. (2008) presented free vibration analysis of composite sandwich plates with soft and honeycomb cores. They obtained the natural frequency of the thin and thick composite sandwich plates using the extended formulation that are consistent with the predictions of the higher-order mixed layerwise theory. Ahn and Lee (2011) studied about transverse vibration characteristics of a sandwich plate with asymmetrical faces. They used the Reissner-Mindlin's plate theory to account the influence of shear deformation and rotary inertia, and derived the equations of motion based on energy method. Mantari *et al*. (2012) developed a new trigonometric shear deformation theory for isotropic, composite laminated and sandwich plates. They employed the principle of virtual work and used Navier's-type solution to derive the governing equations. Also, they showed a very good validation between their model and Reddy's and Touratier's theories. Biaxial buckling analysis of sandwich plates with soft orthotropic core is discussed by Kheirikhah *et al*. (2012). They used the nonlinear geometric Von-Karman relations. Also, the equations of motion and boundary conditions are derived by the principle of minimum potential energy. A trigonometric zigzag theory for the static analysis of laminated composite and sandwich plates is studied by Sahoo and Singh (2014). They demonstrated a very close results with three dimensional elasticity solution. Grover *et al*. (2013) illustrated inverse hyperbolic shear deformation theory to analyze the free vibration response of laminated composite and sandwich plates. Their results showed that both analytical and finite element (FE) solutions are useful for the prediction of the free vibration response. Wang and Shen (2012) studied the nonlinear vibration and bending analysis of sandwich plates with carbon nanotube (CNT) reinforced composite

*Corresponding author, Associate Professor
E-mail: mmohammadimehr@kashanu.ac.ir

ISSN: 1225-4568 (Print), 1598-6217 (Online)

facesheets. They used two-step perturbation technique for solving governing equations. A detailed parametric of their study conducted to investigate the effects of nanotube volume fraction, core-to-face sheet thickness ratio, temperature change, foundation stiffness and in-plane boundary conditions on the nonlinear vibration characteristics. Natarajan *et al.* (2014) presented application of higher-order structural theory to bending and free vibration analysis of sandwich plates with CNT reinforced composite factsheets. They found that the in-plane stress variation is nonlinear and has discontinuity at the layer interface and by raising the volume fraction of CNT distribution in the factsheet, decline the deflection. Static behavior of visco-elastic sandwich plate with composite facesheet under mechanical load is investigated by Kavalur *et al*. (2014). They observed that the maximum static bending deflection of the visco-elastic sandwich plate decreases with an increase in amount fraction of CNTs. Also, thickness and material of visco-elastic core are effective on static behavior. Sayyad and Ghugal (2015) reviewed the recent works done on the free vibration analysis of multilayered laminated composite and sandwich plates. They compared the obtained results by considering various shear deformation theories for displacement fields of these structures. Ghorbanpour Arani *et al*. (2016b) analyzed electro-magneto wave propagation of viscoelastic sandwich nanoplates. They developed the quasi-3D sinusoidal shear deformation plate theory for the sandwich structure contains a single layered graphene sheet as core with zinc oxide facesheets. Also, they used Kelvin-Voigt and Gurtin-Murdoch theories to assume structural damping and surface effects, respectively and an exact solution utilized to determine the natural, cut-off and escape frequencies.

There are many worthwhile works in the case of functionally graded (FG) plates study in literature (Lei *et al*. 2014, Zhang *et al*. 2014, Zhu *et al*. 2014, Lei *et al*. 2015a, Lei *et al*. 2015b, Zhang *et al*. 2015a, Zhang *et al*. 2015b, Zhang *et al*. 2015c, Zhang *et al*. 2015d, Zhang *et al*. 2015e, Zhang *et al*. 2015f, Zhang and Liew 2015a, Zhang and Liew 2015b, Lei *et al*. 2016, Zhang *et al*. 2016a, Zhang *et al*. 2016b, Zhang *et al*. 2016c, Zhang *et al*. 2016d, Zhang *et al*. 2016e, Zhang *et al*. 2016f, Zhang *et al*. 2016g, Zhang *et al*. 2016h, Zhang *et al*. 2016i, Zhang and Liew 2016a, Zhang and Liew 2016b, Liew *et al*. 2017, Viet *et al*. 2017, Zhang *et al*. 2017, Zhang 2017a, Zhang 2017b, Zhang 2017c). Apart from these cases, Zenkor (2005) studied the buckling and free vibration of the simply supported FG sandwich plate by the sinusoidal shear deformation plate theory (SSDT). He investigated the influences of the transverse shear deformation, aspect ratio, side to thickness ratio and volume fraction distributions on the natural frequency and critical buckling load. Free vibration analysis of FG plates using higher order sandwich panel theory is presented by Liu *et al*. (2015). They considered both FG facesheets and FG flexible core by assuming that FG material properties follow a power-law function and demonstrated the influence of distribution of FG material properties, thickness to side ratio on the natural frequencies in their research. Kiani and Eslami (2012) investigated the post-buckling behavior of sandwich plates with FG material facesheets under uniform temperature which is placed on Pasternak-type of elastic foundation. To obtain the equilibrium and compatibility equations of imperfect sandwich plates, they employed the non-linear von-Karman strain-displacement relations. Also, they utilized the single mode approach combined with Galerkin technique to determine the critical buckling temperature and post-buckling equilibrium path of the plate. The bending response of sandwich plates subjected to thermo-mechanical loadings is studied by Zenkour and Alghamdi (2010). To show the effect of material distribution on the deflections and stresses, they employed several theories such as sinusoidal, third-order, first-order shear deformation theories, and classical theory. Then, they demonstrated the influences of thermo-mechanical loadings on the deflections, axial and transverse shear stresses of FG sandwich plate. Buckling analysis of the FG sandwich rectangular plates integrated with piezoelectric layers under bi-axial loads is demonstrated by Arefi (2016). He considered non-homogeneous index of the material properties for sandwich plate and showed that this parameter has important influence on the buckling loads. A three-unknown non-polynomial shear deformation theory for the buckling and vibration analyses of FG sandwich plates is presented by Tounsi *et al*. (2016). They considered the non-linear in plane displacement and constant transverse displacement through the plate thickness in their theory so that it does not need to shear correction factor. Mohammadimehr and Mostafavifar (2016) studied the free vibration of sandwich plate with a transversely flexible core and FG-CNTs reinforced nanocomposite facesheets under one-dimensional (1D) magnetic field using a high-order sandwich plate theory (HSPT). They assumed that mechanical properties of the core are function of temperature and according to this, analyzed the effects of temperature changes on the natural frequency. Also, in their results, it can be seen the natural frequencies increase by applying the magnetic field. Finally, Daouadji and Adim (2017) investigated mechanical behavior of FG sandwich plates using a quasi-3D higher order shear and normal deformation theory. They considered a hyperbolic and parabolic shear and normal deformation theory for the bending analysis to study the effect of thickness stretching in FG sandwich plates.

The study of the researches indicates that there is not any work about double-bonded sandwich microplates with nanocomposite facesheets reinforced by symmetric and un-symmetric distributions of nanotubes under multi physical fields which resting on visco-Pasternak-type of elastic foundation. Investigation of this matter can be much helped to more accurate analysis of micro-electro-mechanical (MEM) and nano-electro-mechanical (NEM) devices. Also, the various distributions of carbon nanotube (CNT) and boron nitride nanotube (BNNT) are considered for nanocomposite facesheets. 2D magnetic fields are applied on CNT reinforced composite facesheets and electric field is applied on BNNT reinforced composite facesheets. Because of the importance of shear deformations in thicker sandwich microplate and require high precision in this

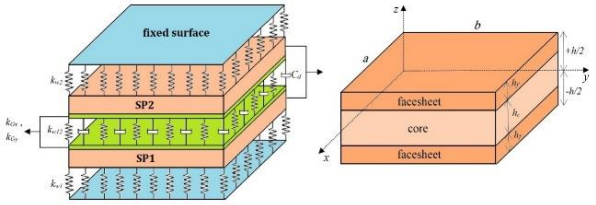

Fig. 1 Schematic of double bonded sandwich microplates embedded in visco-Pasternak medium and rested on Winkler foundation from both sides

system, sinusoidal shear deformation plate theory (SSDT) are considered. Also, modified strain gradient theory (MSGT) is a proper approach to investigate the micro-structures at micro scale which is employed to obtain strain energy of sandwich microplates. Finally, the governing equations are obtained using Hamilton's principle and solved by Navier's approach.

2. Double-bonded FG sandwich microplates

Consider double-bonded sandwich microplates with length a, width b and thickness h as shown schematically in Fig. 1. Sandwich microplates consist of homogenous core with thickness h_c and nanocomposite facesheets with thickness h_f ($h=h_c+2h_f$). To derive the governing equations of motion, the main assumptions are considered as follows (Marynowski 2012):

- The core is thicker and softer than the facesheets.
- No slipping occurs at the interfaces between the core and facesheets.
- The core and facesheets are fully bonded. Therefore, the displacements in $z=+h_c/2$ and $z=-h_c/2$ are the same for core-top facesheet and core-bottom facesheet, respectively.

Bottom sandwich microplate (SP1) and top sandwich microplate (SP2) are made of CNT and BNNT reinforced composite facesheets, respectively. nanocomposite facesheets of SP1 are subjected to the 2D magnetic field which is applied as longitudinal and transverse. Also, piezoelectric nanocomposite facesheets of SP2 are subjected to the electric field which is applied along the thickness. Sandwich microplates are coupled with visco-Pasternak medium and they are rested on Winkler foundation from both sides. The Cartesian coordinate system is selected for this problem as well as the origin is located at the corner of the plate on the middle plane.

In this paper, six-type distributions of nanotubes (CNT and BNNT) are considered for two sandwich plates as shown in Fig. 2. Symmetric distributions are assumed as: uniform distribution (UU) and FG distributions including FG-OO and FG-XX, and un-symmetric distributions are considered as: FG-UO, FG-UX and FG-XO, where each types can be defined with volume fraction of own as follows (Mohammadimehr *et al*. 2016c)

For top facesheet ($\frac{h_c}{2} \le z \le \frac{h_c}{2}+h_f$)

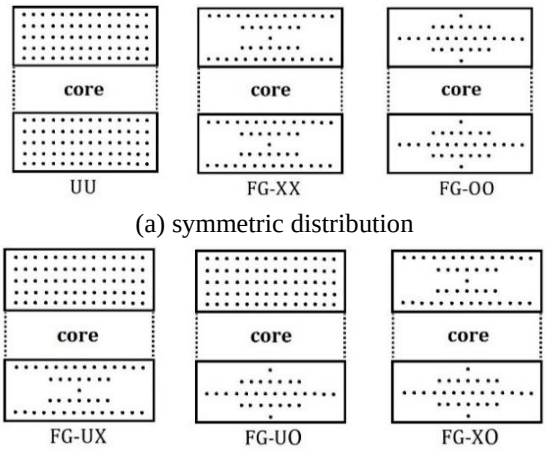

(a) symmetric distribution

(b) un-symmetric distribution

Fig. 2 Various distributions of nanotubes for composite facesheets of sandwich microplate

$$V_{NT}^{t}=\begin{cases} V_{NT}^{*} & U \\ \left(2-\frac{4}{h_f}\left|z-\frac{h_c+h_f}{2}\right|\right)V_{NT}^{*} & FG-O \\ \frac{4}{h_f}\left|z-\frac{h_c+h_f}{2}\right|V_{NT}^{*} & FG-X \end{cases} \tag{1a}$$

For bottom facesheet ($-\frac{h_c}{2}-h_f \le z \le -\frac{h_c}{2}$)

$$V_{NT}^{b}=\begin{cases} V_{NT}^{*} & U \\ \left(2-\frac{4}{h_f}\left|z+\frac{h_c+h_f}{2}\right|\right)V_{NT}^{*} & FG-O \\ \frac{4}{h_f}\left|z+\frac{h_c+h_f}{2}\right|V_{NT}^{*} & FG-X \end{cases} \tag{1b}$$

where:

$$V_{NT}^{*}=\frac{w_{NT}}{w_{NT}+(\rho_{NT}/\rho_M)(1-w_{NT})},$$

in which, w and ρ are called the mass fraction and mass density, respectively. It should be noted that subscripts NT and M are utilized to introduce nanotube and matrix, respectively.

The extended rule of mixture (Esawi and Farag 2007) is a simple and convenient way to estimate the effective material properties of the two-phase composites. This rule can be written as

$$E_{11}=\eta_1 V_{NT}^{t,b} E_{11NT}+V_M E_{11M}, \tag{2a}$$

$$\frac{\eta_2}{E_{22}}=\frac{V_{NT}^{t,b}}{E_{22NT}}+\frac{V_M}{E_{22M}}, \tag{2b}$$

$$\frac{\eta_3}{G_{12}}=\frac{V_{NT}^{t,b}}{G_{12NT}}+\frac{V_M}{G_M}, \tag{2c}$$

$$\nu_{12} = V_{NT}^{*}\nu_{12NT} + V_M \nu_M, \tag{2d}$$

$$\rho = V_{NT}^{t,b}\rho_{NT} + V_M \rho_M, \tag{2e}$$

where η_i (i=1,2,3) are the efficiency parameters and ν is Poisson's ratio. Also, E_{11}, E_{22} and G indicate longitudinal, transversely elastic moduli and shear modulus, respectively. The efficiency parameters for CNTs are defined. These values are obtained by molecular dynamics simulations (Han and Elliott 2007). Since these values have not yet been calculated for BNNTs, based on Mohammadimehr *et al*. (2016a), we had to consider these values for BNNTs. Mohammadimehr *et al*. (2016a) in their paper assumed the values for BNNTs and there is not any value for BNNTs in the literature based on molecular dynamics.

3. Constitutive equations

In this paper, because of the importance of shear deformations in thicker sandwich microplate and require high precision in this system, sinusoidal shear deformation plate theory (SSDT) are considered. The displacement fields for sandwich microplates can be expressed as (Mohammadimehr *et al.* 2015)

$$\begin{aligned} U(x,y,z,t) &= u(x,y,t) - z\frac{\partial w(x,y,t)}{\partial x} + \psi(z)\phi_x(x,y,t), \\ V(x,y,z,t) &= v(x,y,t) - z\frac{\partial w(x,y,t)}{\partial y} + \psi(z)\phi_y(x,y,t), \\ W(x,y,z,t) &= w(x,y,t), \end{aligned} \tag{3}$$

where u, v and w are the displacement components of microplate along the x, y and z axes, respectively, and $\psi(z)$ is equal to $\frac{h}{\pi}\sin(\frac{\pi z}{h})$ for SSDT and if $\psi(z)$ is equal to zero, the displacement fields are obtained for classical plate theory (CPT). Also, ϕ_x and ϕ_y describe the rotational about x and y axes, respectively.

Based on Eq. (3) and displacement-strain relations, the kinematic equations for double-bonded nanocomposite sandwich microplates can be obtained as

$$\begin{Bmatrix} \varepsilon_{xx} \\ \varepsilon_{yy} \\ \gamma_{xy} \end{Bmatrix} = \begin{Bmatrix} \frac{\partial u}{\partial x} \\ \frac{\partial v}{\partial y} \\ \frac{\partial u}{\partial y} + \frac{\partial v}{\partial x} \end{Bmatrix} + z\begin{Bmatrix} -\frac{\partial^2 w}{\partial x^2} \\ -\frac{\partial^2 w}{\partial y^2} \\ -2\frac{\partial^2 w}{\partial x\,\partial y} \end{Bmatrix} + \psi(z)\begin{Bmatrix} \frac{\partial \phi_x}{\partial x} \\ \frac{\partial \phi_y}{\partial y} \\ \frac{\partial \phi_x}{\partial y} + \frac{\partial \phi_y}{\partial x} \end{Bmatrix},$$
$$\begin{Bmatrix} \gamma_{xz} \\ \gamma_{yz} \end{Bmatrix} = \frac{\partial \psi(z)}{\partial z}\begin{Bmatrix} \phi_x \\ \phi_y \end{Bmatrix}, \tag{4}$$

in which, ε and γ are normal and shear strains, respectively. Also, ε_{zz} is obtained equal to zero.

Therefore, the constitutive equations can be written in the following form

$$\begin{Bmatrix} \sigma_{xx} \\ \sigma_{yy} \\ \sigma_{xy} \\ \sigma_{yz} \\ \sigma_{xz} \\ D_x \\ D_y \\ D_z \end{Bmatrix} = \begin{bmatrix} Q_{11} & Q_{12} & 0 & 0 & 0 & 0 & 0 & -e_{31} \\ Q_{12} & Q_{22} & 0 & 0 & 0 & 0 & 0 & -e_{32} \\ 0 & 0 & Q_{66} & 0 & 0 & 0 & 0 & 0 \\ 0 & 0 & 0 & Q_{44} & 0 & 0 & -e_{24} & 0 \\ 0 & 0 & 0 & 0 & Q_{55} & -e_{15} & 0 & 0 \\ 0 & 0 & 0 & 0 & e_{15} & \in_{11} & 0 & 0 \\ 0 & 0 & 0 & e_{24} & 0 & 0 & \in_{22} & 0 \\ e_{31} & e_{32} & 0 & 0 & 0 & 0 & 0 & \in_{33} \end{bmatrix} \begin{Bmatrix} \varepsilon_{xx} \\ \varepsilon_{yy} \\ \gamma_{xy} \\ \gamma_{yz} \\ \gamma_{xz} \\ E_x \\ E_y \\ E_z \end{Bmatrix}, \tag{5}$$

where:

$$Q_{11} = \frac{E_{11}}{1-\nu_{12}\nu_{21}},\ Q_{12} = \frac{\nu_{12}E_{11}}{1-\nu_{12}\nu_{21}},\ Q_{22} = \frac{E_{22}}{1-\nu_{12}\nu_{21}},$$
$$Q_{66} = G_{12},\ Q_{44} = G_{23},\ Q_{55} = G_{13},$$

σ and Q are classical stresses and the material constants, respectively. Also, D_i is the electric displacement and E_i is the electric field components. It should be noted that recent two parameters (D_i and E_i) are equal to zero for SP1.

4. Two dimensional magnetic fields

The Lorentz force, f=(f_x, f_y, f_z), induced by the two-dimensional (2D) magnetic fields, can be determined based on Maxwell's relations as follows (Kraus 1984)

$$J = \nabla \times h, \tag{6}$$

$$\nabla \times e = -\eta\frac{\partial h}{\partial t}, \tag{7}$$

$$\nabla \cdot h = 0, \tag{8}$$

$$e = -\eta\left(\frac{\partial U}{\partial t} \times H\right), \tag{9}$$

$$h = \nabla \times (U \times H), \tag{10}$$

$$f = \eta(J \times H), \tag{11}$$

where J, e and h denote current density, strength vectors of the electric field and distributing vector of the magnetic field, respectively. Also, $\vec{U} = (U,V,W)$ is the displacement vector, η is the magnetic field permeability, and $\nabla = (\partial/\partial x, \partial/\partial y, \partial/\partial z)$ is the Hamiltonian operator.

To determine the Lorentz force, equations are solved once for the longitudinal magnetic field as a vector H=(H_x, 0,0) and once again for transverse magnetic field as a vector H=(0, H_y, 0). Then, by using superposition principle, the Lorentz force applied to SP1 can be calculated by using Eqs. (6)-(11) as the following form

$$\begin{aligned} f_x &= \eta H_y^{\,2}\frac{\partial^3 W}{\partial z\,\partial x} + \eta H_y^{\,2}\frac{\partial^2 U}{\partial x^2} + \eta H_y^{\,2}\frac{\partial^2 U}{\partial y^2}, \\ f_y &= \eta H_x^{\,2}\frac{\partial^3 V}{\partial x^2} + \eta H_x^{\,2}\frac{\partial^3 V}{\partial y^2} + \eta H_x^{\,2}\frac{\partial^3 W}{\partial z\,\partial y}, \\ f_z &= \eta H_x^{\,2}\frac{\partial^3 V}{\partial z\,\partial y} + \eta H_x^{\,2}\frac{\partial^3 W}{\partial z^2} + \eta H_x^{\,2}\frac{\partial^3 W}{\partial x^2} \\ &\quad + \eta H_y^{\,2}\frac{\partial^3 W}{\partial y^2} + \eta H_y^{\,2}\frac{\partial^3 W}{\partial z^2} + \eta H_y^{\,2}\frac{\partial^2 U}{\partial z\,\partial x}. \end{aligned} \tag{12}$$

The virtual external work done due to the 2D magnetic fields can be written as

$$\Sigma_1 = \frac{1}{2}\int_V \left(f_x \cdot U_1 + f_y \cdot V_1 + f_z \cdot W_1\right) dV\,, \tag{13}$$

By substituting Eqs. (3) and (12) into Eq. (13), the external work done due to the 2D magnetic field can be obtained for facesheets of SP1.

5. Electric field

To satisfy the electric potential boundary conditions along the thickness direction, a sinusoidal distribution of the electric potential is considered for facesheets of SP2 as follows (Hosseini Hashemi *et al.* 2010)

$$\Phi(x,y,z,t) = \begin{cases} \sin\left(\dfrac{\pi(z-h_c/2)}{h_f}\right)\varphi(x,y,t) & \dfrac{h_c}{2} < z < \dfrac{h_c}{2}+h_f \\ \sin\left(\dfrac{\pi(-z-h_c/2)}{h_f}\right)\varphi(x,y,t) & -\dfrac{h_c}{2}-h_f < z < -\dfrac{h_c}{2} \end{cases}, \tag{14}$$

where $\varphi(x,y,t)$ is the spatial and time variation of the electric potential caused by bending. Using Eq. (14), the electric field components is derived as follows (Mohammadimehr *et al.* 2016b)

$$E_k = -\frac{\partial\Phi}{\partial x_k} \quad (x_k = x,y,z) \rightarrow \begin{cases} E_x = -\dfrac{\partial\Phi}{\partial x}, \\ E_y = -\dfrac{\partial\Phi}{\partial y}, \\ E_z = -\dfrac{\partial\Phi}{\partial z}. \end{cases} \tag{15}$$

6. Visco-Pasternak of elastic foundation

In this study, it is assumed that SP1 and SP2 are coupled with visco-Pasternak medium and from both sides, they are attached to Winkler foundation. Thus, the effects of foundation are considered as an external force which applied on the sandwich microplates as follows (Ghorbanpour Arani and Amir 2013)

$$\begin{aligned} F_1 = &-k_{w1}W_1 + k_{w12}(W_2 - W_1) + C_d\frac{\partial}{\partial t}(W_2 - W_1) \\ &- k_{Gx}\frac{\partial^2}{\partial x^2}(W_2 - W_1) - k_{Gy}\frac{\partial^2}{\partial y^2}(W_2 - W_1), \end{aligned} \tag{16a}$$

$$\begin{aligned} F_2 = &-k_{w2}W_2 + k_{w12}(W_1 - W_2) + C_d\frac{\partial}{\partial t}(W_1 - W_2) \\ &- k_{Gx}\frac{\partial^2}{\partial x^2}(W_1 - W_2) - k_{Gy}\frac{\partial^2}{\partial y^2}(W_1 - W_2), \end{aligned} \tag{16b}$$

where k_w is spring modulus and C_d is damping modulus. Also, k_{Gx} and k_{Gy} are shear layer constants along x and y axes, respectively. Note that subscripts 1 and 2 are related to the SP1 and SP2, respectively. The external forces can be expressed as follows

$$\begin{aligned} V_1^{ext} &= \frac{1}{2}\int_A (F_1 \cdot W_1) dA, \\ V_2^{ext} &= \frac{1}{2}\int_A (F_2 \cdot W_2) dA, \end{aligned} \tag{17}$$

7. Governing equations of double bonded sandwich micro-plates

Using Hamilton's principle (Ghorbanpour Arani *et al.* 2016a), the equations of motion for double bonded sandwich micro-plates are derived as the following form

$$\begin{aligned} \delta\Pi &= \delta\int_{t_1}^{t_2} (\Pi_{SP1} + \Pi_{SP2}) dt \\ &= \delta\int_{t_1}^{t_2} \left[\left(U_1 - K_1 - V_1^{ext} - \Sigma_1\right) + \left(U_2 - K_2 - V_2^{ext}\right)\right] dt = 0, \end{aligned} \tag{18}$$

in which, U and K present strain and kinetic energies, respectively. Based on MSGT, strain energy for sandwich microplates can be given by (Mohammadimehr *et al.* 2016c)

$$U = \frac{1}{2}\int_V \left(\sigma_{ij}\varepsilon_{jk} + p_i\gamma_i + \tau_{ijk}^{(1)}\eta_{ijk}^{(1)} + m_{ij}\chi_{ij} - D_iE_i\right) dV\,, \tag{19}$$

in which, γ_i, $\eta_{ijk}^{(1)}$ and χ_{ij} represent the dilatation gradient vector, deviatoric stretch gradient and symmetric rotation gradient tensors, respectively, and their corresponding terms (p_i, $\tau_{ijk}^{(1)}$ and m_{ij}) are the higher-order stresses.

$$\varepsilon_{ij} = \frac{1}{2}\left(\frac{\partial u_j}{\partial x_i} + \frac{\partial u_i}{\partial x_j}\right), \tag{20a}$$

$$\gamma_i = \frac{\partial\varepsilon_{mm}}{\partial x_i}, \tag{20b}$$

$$\begin{aligned} \eta_{ijk}^{(1)} = &\frac{1}{3}\left(\frac{\partial\varepsilon_{jk}}{\partial x_i} + \frac{\partial\varepsilon_{ki}}{\partial x_j} + \frac{\partial\varepsilon_{ij}}{\partial x_k}\right) - \frac{1}{15}\delta_{ij}\left(\frac{\partial\varepsilon_{mm}}{\partial x_k} + 2\frac{\partial\varepsilon_{mk}}{\partial x_m}\right) \\ &- \frac{1}{15}\delta_{jk}\left(\frac{\partial\varepsilon_{mm}}{\partial x_i} + 2\frac{\partial\varepsilon_{mi}}{\partial x_m}\right) - \frac{1}{15}\delta_{ki}\left(\frac{\partial\varepsilon_{mm}}{\partial x_j} + 2\frac{\partial\varepsilon_{mj}}{\partial x_m}\right), \end{aligned} \tag{20c}$$

$$\chi_{ij} = \frac{1}{2}\left(e_{ipq}\frac{\partial\varepsilon_{qj}}{\partial x_p} + e_{jpq}\frac{\partial\varepsilon_{qi}}{\partial x_p}\right), \tag{20d}$$

$$p_i = 2l_0^2 G\gamma_i, \tag{21a}$$

$$\tau_{ijk}^{(1)} = 2l_1^2 G\eta_{ijk}^{(1)}, \tag{21b}$$

$$m_{ij} = 2l_2^2 G\chi_{ij}, \tag{21c}$$

In Eqs. (20), u_i, δ_{ij} and e_{ipq} denote the displacement vector, kronecker delta and alternate tensor, respectively. Also, in Eq. (21), l_0, l_1, and l_2 denote three additional independent material length scale parameters associated with the dilatation gradients, deviatoric stretch gradients and symmetric rotation gradients, respectively. If the parameters l_0 and l_1 should be equal to zero, then the modified strain gradient theory (MSGT) in Eq. (21) is converted to the modified couple stress theory (MCST). Also, if three material length scale parameters should be equal to zero, then the classical theory is obtained. Thus, there is a discrepancy between the results of different theories including MSGT(l_0,l_1,l_2≠0), MCST (l_0=l_1=0), and CT (l_0=l_1=l_2=0).

By expanding Eqs. (20) and substituting Eq. (4) into this equation, the results can be obtained according to Appendix A.

Kinetic energy of sandwich microplates can be expressed as follows

$$K_1 = \int_V \frac{1}{2}\rho_1\left(\left(\frac{\partial U}{\partial t}\right)^2+\left(\frac{\partial V}{\partial t}\right)^2+\left(\frac{\partial W}{\partial t}\right)^2\right)dV,$$
$$K_2 = \int_V \frac{1}{2}\rho_2\left(\left(\frac{\partial U}{\partial t}\right)^2+\left(\frac{\partial V}{\partial t}\right)^2+\left(\frac{\partial W}{\partial t}\right)^2\right)dV. \tag{22}$$

Substituting Eqs. (13), (17), (19), and (22) into Eq. (18), the equations of motion for double-bonded sandwich microplates with FG nanocomposite facesheets under 2D magnetic and electric fields can be calculated. To change the equations of motion in a dimensionless form, the following parameters including geometric, mechanical and electrical parameters are defined

$$(X,Y,W)=\left(\frac{x}{a},\frac{y}{b},\frac{w}{h}\right),\ (\alpha,\beta,\overline{l_i})=\left(\frac{h}{a},\frac{a}{b},\frac{l_i}{a}\right)(i=0,1,2),$$
$$\tau=\frac{t}{a}\sqrt{\frac{A_{11}^{c-s}}{h^3\rho^{c-s}}},\ \ \bar{\varphi}=\frac{a^2e_{31}\varphi}{A_{11}^{c-s}},\ \ \bar{\in}=\frac{A_{11}^{c-s}\in}{a^3e_{31}^{\ 2}},\bar{e}=\frac{e}{e_{31}},$$
$$\overline{G_j^s}=\frac{G_j^s}{A_{11}^{c-s}}(j=2,3,4),\ \overline{G_k^s}=\frac{G_k^sa^2}{A_{11}^{c-s}}(k=0,5,6,7,9),\ \overline{G_8^s}=\frac{G_8^sa^4}{A_{11}^{c-s}},$$
$$\overline{A^s},\overline{B^s},\overline{D^s}=\frac{A^s,B^s,D^s}{A_{11}^{c-s}},\overline{I_0^s}=\frac{I_0^sa^2}{h^3\rho^{c-s}},\ \overline{I_j^s}=\frac{I_j^s}{h^3\rho^{c-s}},\overline{C_{44,55}^s}=\frac{C_{44,55}^sa^2}{A_{11}^{c-s}},$$
$$\overline{S_{1,5}}=\frac{S_{1,5}}{a},\ \overline{S_j}=\frac{S_j}{a^3},\ H_x^*=\eta H_x\sqrt{\frac{a^3}{A_{11}^{c-s}}},H=\frac{H_y^*}{H_x^*},\ \overline{P_{1,5}}=\frac{P_{1,5}}{h^2},$$
$$\overline{P_j}=\frac{P_j}{h},\ k_{w12}^*=\frac{k_{w12}a^4}{A_{11}^{c-s}},\ k_1=\frac{k_{w1}^*}{k_{w12}^*},\ k_2=\frac{k_{w2}^*}{k_{w12}^*},C_d^*=C_da^2\sqrt{\frac{1}{hA_{11}^{c-s}\rho^{c-s}}},$$
$$k_{Gx}^*=\frac{k_{Gx}a^2}{A_{11}^{c-s}},\ k_G=\frac{k_{Gy}^*}{k_{Gx}^*},\ h^*=\frac{h}{h_f}. \tag{23}$$

It should be noted that in Eq. (23), superscript *s* refer to SP1 and SP2. Also, other coefficients are mentioned in Appendix B. Finally, the dimensionless equations of motion for double-bonded sandwich microplates can be determined as follows

$$\begin{aligned}
&\delta w_1 = \\
&-2\overline{l_0^{\,2}}\overline{G_5^1}\beta^2\frac{\partial^3\phi_{x1}}{\partial Y^{\,2}\partial X}-2\overline{l_0^{\,2}}\overline{G_5^1}\beta\frac{\partial^3\phi_{y1}}{\partial Y\partial X^{\,2}}-2\overline{l_0^{\,2}}\overline{G_5^1}\frac{\partial^3\phi_{x1}}{\partial X^3}+2\overline{l_0^{\,2}}\overline{G_3^1}\frac{\partial^5\phi_{x1}}{\partial X^5}\\
&+4\overline{l_0^{\,2}}\overline{G_3^1}\beta^3\frac{\partial^5\phi_{y1}}{\partial Y^{\,3}\partial X^{\,2}}+2\overline{l_0^{\,2}}\overline{G_3^1}\beta^5\frac{\partial^5\phi_{y1}}{\partial Y^5}+2\overline{l_0^{\,2}}\overline{G_3^1}\beta\frac{\partial^5\phi_{y1}}{\partial Y\partial X^4}\\
&+4\overline{l_0^{\,2}}\overline{G_3^1}\beta^2\frac{\partial^5\phi_{x1}}{\partial Y^{\,2}\partial X^3}-6\overline{l_0^{\,2}}\overline{G_2^1}\alpha\beta^4\frac{\partial^4W_1}{\partial Y^{\,4}\partial X^{\,2}}+2\overline{l_0^{\,2}}\overline{G_0^1}\alpha\beta^4\frac{\partial^4W_1}{\partial Y^4}\\
&+\frac{16}{15}\overline{l_0^{\,2}}\overline{G_0^1}\alpha\beta^2\frac{\partial^4W_1}{\partial Y^{\,2}\partial X^{\,2}}+2\overline{l_0^{\,2}}\overline{G_3^1}\beta^4\frac{\partial^5\phi_{x1}}{\partial Y^{\,4}\partial X}-6\overline{l_0^{\,2}}\overline{G_2^1}\alpha\beta^2\frac{\partial^6W_1}{\partial Y^{\,2}\partial X^4}\\
&-2\overline{l_0^{\,2}}\overline{G_2^1}\alpha\beta^6\frac{\partial^6W_1}{\partial Y^6}+4\overline{l_0^{\,2}}\overline{G_0^1}\alpha\beta^2\frac{\partial^4W_1}{\partial Y^{\,2}\partial X^{\,2}}+\frac{8}{15}\overline{l_0^{\,2}}\overline{G_0^1}\alpha\beta^4\frac{\partial^4W_1}{\partial Y^4}\\
&-2\overline{l_0^{\,2}}\overline{G_5^1}\beta^3\frac{\partial^5\phi_{y1}}{\partial Y^3}+2\overline{l_0^{\,2}}\overline{G_0^1}\alpha\frac{\partial^6W_1}{\partial X^4}-2\overline{l_0^{\,2}}\overline{G_2^1}\alpha\frac{\partial^6W_1}{\partial X^6}+\frac{8}{15}\overline{l_0^{\,2}}\overline{G_0^1}\alpha\frac{\partial^6W_1}{\partial X^4}\\
&-\frac{4}{5}\overline{l_1^{\,2}}\overline{G_2^1}\alpha\frac{\partial^6W_1}{\partial X^6}-\frac{2}{5}\overline{l_1^{\,2}}\overline{G_7^1}\beta^2\frac{\partial^5\phi_{x1}}{\partial Y^{\,2}\partial X}+\frac{4}{5}\overline{l_1^{\,2}}\overline{G_3^1}\beta^4\frac{\partial^5\phi_{x1}}{\partial Y^4\partial X}\\
&+\frac{8}{5}\overline{l_1^{\,2}}\overline{G_3^1}\beta^2\frac{\partial^5\phi_{x1}}{\partial Y^{\,2}\partial X^3}+\frac{8}{5}\overline{l_1^{\,2}}\overline{G_3^1}\beta^3\frac{\partial^5\phi_{y1}}{\partial Y^{\,3}\partial X^{\,2}}-\frac{16}{15}\overline{l_1^{\,2}}\overline{G_5^1}\beta^3\frac{\partial^3\phi_{y1}}{\partial Y^3}\\
&-\frac{16}{15}\overline{l_1^{\,2}}\overline{G_5^1}\beta\frac{\partial^3\phi_{y1}}{\partial Y\partial X^{\,2}}-\frac{16}{15}\overline{l_1^{\,2}}\overline{G_5^1}\beta^2\frac{\partial^3\phi_{x1}}{\partial Y^{\,2}\partial X}-\frac{2}{5}\overline{l_1^{\,2}}\overline{G_9^1}\beta\frac{\partial^3\phi_{y1}}{\partial Y\partial X^{\,2}}\\
&+\frac{4}{5}\overline{l_1^{\,2}}\overline{G_3^1}\beta\frac{\partial^5\phi_{y1}}{\partial Y\partial X^4}-\frac{2}{5}\overline{l_1^{\,2}}\overline{G_7^1}\beta^3\frac{\partial^3\phi_{y1}}{\partial Y^3}-\frac{2}{5}\overline{l_1^{\,2}}\overline{G_9^1}\frac{\partial^3\phi_{x1}}{\partial X^3}+\frac{4}{5}\overline{l_1^{\,2}}\overline{G_3^1}\frac{\partial^5\phi_{x1}}{\partial X^5}\\
&-\frac{16}{15}\overline{l_1^{\,2}}\overline{G_5^1}\frac{\partial^3\phi_{x1}}{\partial X^3}-\frac{4}{5}\overline{l_1^{\,2}}\overline{G_2^1}\alpha\beta^6\frac{\partial^6W_1}{\partial Y^6}-\frac{12}{5}\overline{l_1^{\,2}}\overline{G_2^1}\alpha\beta^4\frac{\partial^6W_1}{\partial Y^{\,4}\partial X^{\,2}}\\
&-\frac{12}{5}\overline{l_1^{\,2}}\overline{G_2^1}\alpha\beta^2\frac{\partial^6W_1}{\partial Y^{\,2}\partial X^4}+\frac{4}{5}\overline{l_1^{\,2}}\overline{G_3^1}\beta^5\frac{\partial^5\phi_{y1}}{\partial Y^5}-\frac{1}{4}\overline{l_2^{\,2}}\overline{G_5^1}\beta^3\frac{\partial^3\phi_{y1}}{\partial Y^3}\\
&+\frac{1}{2}\overline{l_2^{\,2}}\overline{G_0^1}\alpha\frac{\partial^6W_1}{\partial X^4}+\frac{1}{2}\overline{l_2^{\,2}}\overline{G_0^1}\alpha\beta^4\frac{\partial^4W_1}{\partial Y^4}+3\overline{l_2^{\,2}}\overline{G_0^1}\alpha\beta^2\frac{\partial^6W_1}{\partial Y^{\,2}\partial X^{\,2}}-\frac{1}{4}\overline{l_2^{\,2}}\overline{G_5^1}\frac{\partial^3\phi_{x1}}{\partial X^3}\\
&-\frac{3}{4}\overline{l_2^{\,2}}\overline{G_5^1}\beta\frac{\partial^3\phi_{y1}}{\partial Y\partial X^{\,2}}-\frac{3}{4}\overline{l_2^{\,2}}\overline{G_5^1}\beta^2\frac{\partial^3\phi_{x1}}{\partial Y^{\,2}\partial X}+4\overline{A_{66}^1}\alpha\beta^2\frac{\partial^4W_1}{\partial Y^{\,2}\partial X^{\,2}}\\
&+\overline{A_{22}^1}\alpha\beta^4\frac{\partial^4W_1}{\partial Y^4}+2\overline{A_{12}^1}\alpha\beta^2\frac{\partial^4W_1}{\partial Y^{\,2}\partial X^{\,2}}+\overline{A_{11}^1}\alpha\frac{\partial^4W_1}{\partial X^4}-\overline{D_{12}^1}\beta\frac{\partial^3\phi_{y1}}{\partial Y\partial X^{\,2}}\\
&-2\overline{D_{12}^1}\beta^2\frac{\partial^3\phi_{x1}}{\partial Y^{\,2}\partial X}-\overline{D_{22}^1}\beta^3\frac{\partial^3\phi_{y1}}{\partial Y^3}-2\overline{D_{66}^1}\beta^2\frac{\partial^3\phi_{x1}}{\partial Y^{\,2}\partial X}-2\overline{D_{66}^1}\beta\frac{\partial^3\phi_{y1}}{\partial Y\partial X^{\,2}}\\
&-\overline{D_{11}^1}\frac{\partial^3\phi_{x1}}{\partial X^3}+\overline{I_3^1}\frac{\partial^3\phi_{x1}}{\partial\tau^2\partial X}-\overline{I_2^1}\alpha\beta^2\frac{\partial^4W_1}{\partial\tau^2\partial Y^{\,2}}-\overline{I_2^1}\alpha\frac{\partial^4W_1}{\partial\tau^2\partial X^{\,2}}+\overline{I_0^1}\alpha\frac{\partial^4W_1}{\partial\tau^2}\\
&+\overline{I_3^1}\beta\frac{\partial^3\phi_{y1}}{\partial\tau^2\partial Y}-\frac{1}{2}H_x^{*2}\overline{S_5}\beta\frac{\partial\phi_{y1}}{\partial Y}-H_x^{*2}\overline{S_1}\alpha\frac{\partial^3W_1}{\partial X^{\,2}}-H^2H_x^{*2}\overline{S_3}\frac{\partial^3\phi_{x1}}{\partial X^3}\\
&-H_x^{*2}\overline{S_3}\beta^3\frac{\partial^3\phi_{y1}}{\partial Y^3}-H_x^{*2}\overline{S_3}\beta\frac{\partial^3\phi_{y1}}{\partial Y\partial X^{\,2}}+H^2H_x^{*2}\overline{S_1}\alpha\frac{\partial^3W_1}{\partial X^{\,2}}\\
&+H_x^{*2}\overline{S_2}\alpha\beta^2\frac{\partial^4W_1}{\partial Y^{\,2}\partial X^{\,2}}+H_x^{*2}\overline{S_2}\alpha\beta^4\frac{\partial^4W_1}{\partial Y^4}-H^2H_x^{*2}\overline{S_3}\beta^2\frac{\partial^3\phi_{x1}}{\partial Y^{\,2}\partial X}\\
&+H^2H_x^{*2}\overline{S_2}\alpha\frac{\partial^4W_1}{\partial X^4}+H_x^{*2}\overline{S_1}\alpha\beta^2\frac{\partial^4W_1}{\partial Y^{\,2}}-\frac{1}{2}H^2H_x^{*2}\overline{S_5}\frac{\partial\phi_{x1}}{\partial X}\\
&+H^2H_x^{*2}\overline{S_2}\alpha\beta^2\frac{\partial^4W_1}{\partial Y^{\,2}\partial X^{\,2}}-H^2H_x^{*2}\overline{S_1}\alpha\beta^2\frac{\partial^2W_1}{\partial Y^{\,2}}-\alpha\beta^2k_Gk_{Gx}^*\frac{\partial^2W_1}{\partial Y^{\,2}}\\
&+\alpha\beta^2k_Gk_{Gx}^*\frac{\partial^2W_2}{\partial Y^{\,2}}-\alpha k_{Gx}^*\frac{\partial^2W_1}{\partial X^{\,2}}+\alpha k_{Gx}^*\frac{\partial^2W_2}{\partial X^{\,2}}+C_d^*\frac{\partial W_1}{\partial\tau}-C_d^*\frac{\partial W_2}{\partial\tau}\\
&+\alpha k_1k_{w12}^*W_1-\alpha k_{w12}^*W_2+\alpha k_{w12}^*W_1=0,
\end{aligned} \tag{24a}$$

$$\begin{aligned}
&\delta\phi_{x1} = \\
&2\overline{l_0^{\,2}}\overline{G_4^1}\frac{\partial^4\phi_{x1}}{\partial X^4}-2\overline{l_0^{\,2}}\overline{G_6^1}\frac{\partial^2\phi_{x1}}{\partial X^{\,2}}-2\overline{l_0^{\,2}}\overline{G_3^1}\alpha\frac{\partial^3W_1}{\partial X^5}-2\overline{l_0^{\,2}}\overline{G_6^1}\beta\frac{\partial^2\phi_{y1}}{\partial Y\partial X}\\
&+2\overline{l_0^{\,2}}\overline{G_4^1}\beta^3\frac{\partial^4\phi_{y1}}{\partial Y^{\,3}\partial X}+2\overline{l_0^{\,2}}\overline{G_5^1}\alpha\frac{\partial^4W_1}{\partial X^3}+2\overline{l_0^{\,2}}\overline{G_4^1}\beta\frac{\partial^4\phi_{y1}}{\partial Y\partial X^3}\\
&+2\overline{l_0^{\,2}}\overline{G_4^1}\beta^2\frac{\partial^4\phi_{x1}}{\partial Y^{\,2}\partial X^{\,2}}-4\overline{l_0^{\,2}}\overline{G_3^1}\beta^2\alpha\frac{\partial^3W_1}{\partial Y^{\,2}\partial X^3}-2\overline{l_0^{\,2}}\overline{G_3^1}\beta^4\alpha\frac{\partial^3W_1}{\partial Y^{\,4}\partial X}\\
&+2\overline{l_0^{\,2}}\overline{G_5^1}\beta^2\alpha\frac{\partial^3W_1}{\partial Y^{\,2}\partial X}-\frac{1}{8}\overline{l_1^{\,2}}\overline{G_6^1}\frac{\partial^2\phi_{x1}}{\partial X^2}-\frac{4}{5}\overline{l_1^{\,2}}\overline{G_7^1}\frac{\partial^2\phi_{x1}}{\partial X^2}+\frac{4}{5}\overline{l_1^{\,2}}\overline{G_4^1}\frac{\partial^4\phi_{x1}}{\partial X^4}\\
&-\frac{32}{15}\overline{l_1^{\,2}}\overline{G_6^1}\frac{\partial^2\phi_{x1}}{\partial X^2}+\frac{16}{15}\overline{l_1^{\,2}}\overline{G_5^1}\alpha\frac{\partial^3W_1}{\partial X^3}+\frac{4}{3}\overline{l_1^{\,2}}\overline{G_4^1}\beta^2\frac{\partial^4\phi_{x1}}{\partial Y^{\,2}\partial X^2}-\frac{4}{3}\overline{l_1^{\,2}}\overline{G_6^1}\beta^2\frac{\partial^2\phi_{x1}}{\partial Y^{\,2}}\\
&+\frac{8}{15}\overline{l_1^{\,2}}\overline{G_4^1}\beta^4\frac{\partial^4\phi_{x1}}{\partial Y^4}-\frac{4}{15}\overline{l_1^{\,2}}\overline{G_7^1}\beta^2\frac{\partial^2\phi_{x1}}{\partial Y^{\,2}}-\frac{8}{15}\overline{l_1^{\,2}}\overline{G_7^1}\beta\frac{\partial^2\phi_{y1}}{\partial Y\partial X}-\frac{4}{5}\overline{l_1^{\,2}}\overline{G_3^1}\alpha\frac{\partial^5W_1}{\partial X^5}\\
&+\frac{2}{5}\overline{l_1^{\,2}}\overline{G_9^1}\alpha\frac{\partial^3W_1}{\partial X^3}+\frac{4}{15}\overline{l_1^{\,2}}\overline{G_4^1}\beta\frac{\partial^4\phi_{y1}}{\partial Y\partial X^3}-\frac{4}{5}\overline{l_1^{\,2}}\overline{G_6^1}\beta\frac{\partial^2\phi_{y1}}{\partial Y\partial X}\\
&+\frac{4}{15}\overline{l_1^{\,2}}\overline{G_4^1}\beta^3\frac{\partial^4\phi_{y1}}{\partial Y^{\,3}\partial X}+\frac{8}{15}\overline{l_1^{\,2}}\overline{G_8^1}\phi_{x1}-\frac{8}{5}\overline{l_1^{\,2}}\overline{G_3^1}\beta^2\alpha\frac{\partial^5W_1}{\partial Y^{\,2}\partial X^3}\\
&+\frac{16}{15}\overline{l_1^{\,2}}\overline{G_5^1}\beta^2\alpha\frac{\partial^3W_1}{\partial Y^{\,2}\partial X}+\frac{2}{5}\overline{l_1^{\,2}}\overline{G_7^1}\beta^2\alpha\frac{\partial^3W_1}{\partial Y^{\,2}\partial X}-\frac{4}{5}\overline{l_1^{\,2}}\overline{G_3^1}\beta^4\alpha\frac{\partial^3W_1}{\partial Y^{\,4}\partial X}\\
&-\overline{l_2^{\,2}}\overline{G_6^1}\beta^2\frac{\partial^2\phi_{x1}}{\partial Y^{\,2}}-\frac{1}{8}\overline{l_2^{\,2}}\overline{G_4^1}\beta^3\frac{\partial^4\phi_{y1}}{\partial Y^{\,3}\partial X}+\frac{5}{8}\overline{l_2^{\,2}}\overline{G_6^1}\beta\frac{\partial^2\phi_{y1}}{\partial Y\partial X}+\frac{1}{4}\overline{l_2^{\,2}}\overline{G_7^1}\beta\frac{\partial^2\phi_{y1}}{\partial Y\partial X}\\
&+\frac{1}{4}\overline{l_2^{\,2}}\overline{G_5^1}\alpha\frac{\partial^3W_1}{\partial X^3}-\frac{1}{8}\overline{l_2^{\,2}}\overline{G_4^1}\beta\frac{\partial^4\phi_{y1}}{\partial Y\partial X^3}+\frac{1}{8}\overline{l_2^{\,2}}\overline{G_4^1}\beta^2\frac{\partial^4\phi_{x1}}{\partial Y^{\,2}\partial X^2}+\frac{1}{8}\overline{l_2^{\,2}}\overline{G_4^1}\beta^4\frac{\partial^4\phi_{x1}}{\partial Y^4}\\
&-\frac{1}{4}\overline{l_2^{\,2}}\overline{G_7^1}\beta^2\frac{\partial^2\phi_{x1}}{\partial Y^{\,2}}+\frac{1}{8}\overline{l_2^{\,2}}\overline{G_8^1}\phi_{x1}+\frac{3}{4}\overline{l_2^{\,2}}\overline{G_5^1}\beta^2\alpha\frac{\partial^3W_1}{\partial Y^{\,2}\partial X}+\overline{C_{55}^1}\phi_{x1}-\overline{B_{66}^1}\beta^2\frac{\partial^2\phi_{x1}}{\partial Y^{\,2}}\\
&-\overline{B_{66}^1}\beta\frac{\partial^2\phi_{y1}}{\partial Y\partial X}-\overline{B_{12}^1}\beta\frac{\partial^2\phi_{y1}}{\partial Y\partial X}-\overline{B_{12}^1}\frac{\partial^2\phi_{x1}}{\partial X^{\,2}}+\overline{D_{11}^1}\alpha\frac{\partial^3W_1}{\partial X^3}+2\overline{D_{12}^1}\beta^2\alpha\frac{\partial^3W_1}{\partial Y^{\,2}\partial X}\\
&+2\overline{D_{66}^1}\beta^2\alpha\frac{\partial^3W_1}{\partial Y^{\,2}\partial X}-\overline{I_3^1}\alpha\frac{\partial^3W_1}{\partial\tau^2\partial X}+\overline{I_4^1}\frac{\partial^2\phi_{x1}}{\partial\tau^2}-H^2H_x^{*2}\overline{S_4}\frac{\partial^2\phi_{x1}}{\partial X^2}+\frac{1}{2}H^2H_x^{*2}\overline{S_5}\alpha\frac{\partial W_1}{\partial X}\\
&+H^2H_x^{*2}\overline{S_3}\alpha\frac{\partial^3W_1}{\partial X^3}-H^2H_x^{*2}\overline{S_4}\beta^2\frac{\partial^2\phi_{x1}}{\partial Y^{\,2}}+H^2H_x^{*2}\overline{S_3}\beta^2\alpha\frac{\partial^3W_1}{\partial Y^{\,2}\partial X}=0,
\end{aligned} \tag{24b}$$

$$\begin{aligned}
&\delta\phi_{y1} = \\
&2\overline{l_0^{\,2}}\overline{G_4^1}\beta\frac{\partial^4\phi_{x1}}{\partial Y\partial X^3}-2\overline{l_0^{\,2}}\overline{G_6^1}\beta^2\frac{\partial^2\phi_{y1}}{\partial Y^{\,2}}+2\overline{l_0^{\,2}}\overline{G_4^1}\beta^4\frac{\partial^4\phi_{y1}}{\partial Y^4}+2\overline{l_0^{\,2}}\overline{G_4^1}\beta^2\frac{\partial^4\phi_{y1}}{\partial Y^{\,2}\partial X^{\,2}}\\
&+2\overline{l_0^{\,2}}\overline{G_4^1}\beta^3\frac{\partial^4\phi_{x1}}{\partial Y^{\,3}\partial X}-2\overline{l_0^{\,2}}\overline{G_6^1}\beta\frac{\partial^2\phi_{x1}}{\partial Y\partial X}+2\overline{l_0^{\,2}}\overline{G_5^1}\alpha\beta^3\frac{\partial^3W_1}{\partial Y^3}+2\overline{l_0^{\,2}}\overline{G_5^1}\alpha\beta\frac{\partial^3W_1}{\partial Y\partial X^{\,2}}\\
&-2\overline{l_0^{\,2}}\overline{G_3^1}\alpha\beta^5\frac{\partial^3W_1}{\partial Y^5}-2\overline{l_0^{\,2}}\overline{G_3^1}\alpha\beta\frac{\partial^3W_1}{\partial Y\partial X^4}-4\overline{l_0^{\,2}}\overline{G_3^1}\alpha\beta^3\frac{\partial^3W_1}{\partial Y^{\,3}\partial X^{\,2}}+\frac{8}{15}\overline{l_1^{\,2}}\overline{G_4^1}\frac{\partial^4\phi_{y1}}{\partial X^4}\\
&-\frac{4}{3}\overline{l_1^{\,2}}\overline{G_6^1}\frac{\partial^2\phi_{y1}}{\partial X^2}-\frac{4}{15}\overline{l_1^{\,2}}\overline{G_7^1}\frac{\partial^2\phi_{y1}}{\partial X^2}+\frac{8}{15}\overline{l_1^{\,2}}\overline{G_8^1}\phi_{y1}+\frac{4}{15}\overline{l_1^{\,2}}\overline{G_4^1}\beta\frac{\partial^4\phi_{x1}}{\partial Y\partial X^3}\\
&+\frac{4}{3}\overline{l_1^{\,2}}\overline{G_4^1}\beta^2\frac{\partial^4\phi_{y1}}{\partial Y^{\,2}\partial X^{\,2}}+\frac{4}{5}\overline{l_1^{\,2}}\overline{G_4^1}\beta^4\frac{\partial^4\phi_{y1}}{\partial Y^4}-\frac{4}{5}\overline{l_1^{\,2}}\overline{G_7^1}\beta^2\frac{\partial^2\phi_{y1}}{\partial Y^{\,2}}-\frac{8}{15}\overline{l_1^{\,2}}\overline{G_7^1}\beta\frac{\partial^2\phi_{x1}}{\partial Y\partial X}\\
&-\frac{4}{5}\overline{l_1^{\,2}}\overline{G_6^1}\beta\frac{\partial^2\phi_{x1}}{\partial Y\partial X}-\frac{32}{15}\overline{l_1^{\,2}}\overline{G_6^1}\beta^2\frac{\partial^2\phi_{y1}}{\partial Y^{\,2}}-\frac{4}{5}\overline{l_1^{\,2}}\overline{G_3^1}\alpha\beta\frac{\partial^4W_1}{\partial Y\partial X^4}+\frac{2}{5}\overline{l_1^{\,2}}\overline{G_7^1}\alpha\beta^3\frac{\partial^3W_1}{\partial Y^3}\\
&+\frac{4}{15}\overline{l_1^{\,2}}\overline{G_4^1}\alpha\beta^3\frac{\partial^4\phi_{x1}}{\partial Y^{\,3}\partial X}-\frac{4}{5}\overline{l_1^{\,2}}\overline{G_3^1}\alpha\beta^5\frac{\partial^3W_1}{\partial Y^5}+\frac{16}{15}\overline{l_1^{\,2}}\overline{G_5^1}\alpha\beta^3\frac{\partial^3W_1}{\partial Y^3}\\
&-\frac{8}{5}\overline{l_1^{\,2}}\overline{G_3^1}\alpha\beta^3\frac{\partial^3W_1}{\partial Y^{\,3}\partial X^{\,2}}+\frac{16}{15}\overline{l_1^{\,2}}\overline{G_5^1}\alpha\beta\frac{\partial^3W_1}{\partial Y\partial X^{\,2}}+\frac{2}{5}\overline{l_1^{\,2}}\overline{G_9^1}\alpha\beta\frac{\partial^3W_1}{\partial Y\partial X^{\,2}}\\
&+\frac{3}{4}\overline{l_2^{\,2}}\overline{G_5^1}\alpha\beta\frac{\partial^3W_1}{\partial Y\partial X^{\,2}}+\frac{1}{4}\overline{l_2^{\,2}}\overline{G_5^1}\alpha\beta^3\frac{\partial^3W_1}{\partial Y^3}-\frac{1}{8}\overline{l_2^{\,2}}\overline{G_6^1}\beta^2\frac{\partial^2\phi_{y1}}{\partial Y^{\,2}}+\frac{1}{8}\overline{l_2^{\,2}}\overline{G_4^1}\frac{\partial^4\phi_{y1}}{\partial X^4}\\
&-\overline{l_2^{\,2}}\overline{G_6^1}\frac{\partial^2\phi_{y1}}{\partial X^2}-\frac{1}{4}\overline{l_2^{\,2}}\overline{G_7^1}\frac{\partial^2\phi_{y1}}{\partial X^2}+\frac{1}{8}\overline{l_2^{\,2}}\overline{G_8^1}\phi_{y1}+\frac{1}{4}\overline{l_2^{\,2}}\overline{G_7^1}\beta\frac{\partial^2\phi_{x1}}{\partial Y\partial X}+\frac{5}{8}\overline{l_2^{\,2}}\overline{G_6^1}\beta\frac{\partial^2\phi_{x1}}{\partial Y\partial X}
\end{aligned} \tag{24c}$$

$$
\begin{aligned}
&-\frac{1}{8}\overline{I_2}^2\overline{G_4^1}\beta^3\frac{\partial^4\phi_{x1}}{\partial Y^3\partial X}-\frac{1}{8}\overline{I_2}^2\overline{G_4^1}\beta\frac{\partial^4\phi_{x1}}{\partial Y\partial X^3}+\frac{1}{8}\overline{I_2}^2\overline{G_4^1}\beta^2\frac{\partial^4\phi_{y1}}{\partial Y^2\partial X^2}+\overline{C_{44}^1}\phi_{y1}\\
&-\overline{B_{66}^1}\beta\frac{\partial^2\phi_{x1}}{\partial Y\partial X}-\overline{B_{12}^1}\beta\frac{\partial^2\phi_{x1}}{\partial Y\partial X}-\overline{B_{22}^1}\beta^2\frac{\partial^2\phi_{y1}}{\partial Y^2}-\overline{B_{66}^1}\frac{\partial^2\phi_{y1}}{\partial X^2}+\overline{D_{22}^1}\alpha\beta^3\frac{\partial W_1}{\partial Y^3}\\
&+2\overline{D_{66}^1}\alpha\beta\frac{\partial^3W_1}{\partial Y\partial X^2}+\overline{D_{12}^1}\alpha\beta\frac{\partial^3W_1}{\partial Y\partial X^2}+\overline{I_4^1}\frac{\partial^2\phi_{y1}}{\partial\tau^2}-\overline{I_3^1}\alpha\beta\frac{\partial^3W_1}{\partial\tau^2\partial Y}-H_x^{*2}\overline{S_4}\frac{\partial^2\phi_{y1}}{\partial X^2}\\
&-H_x^{*2}\overline{S_4}\beta^2\frac{\partial^2\phi_{y1}}{\partial Y^2}+H_x^{*2}\overline{S_3}\alpha\beta^3\frac{\partial W_1}{\partial Y^3}+H_x^{*2}\overline{S_3}\alpha\beta\frac{\partial^3W_1}{\partial Y\partial X^2}+\frac{1}{2}H_x^{*2}\overline{S_5}\alpha\beta\frac{\partial W_1}{\partial Y}=0,
\end{aligned}
$$

$\delta w_2 =$

$$
\begin{aligned}
&-2\overline{l_0}^2\overline{G_5^2}\beta^2\frac{\partial^3\phi_{x2}}{\partial Y^2\partial X}-2\overline{l_0}^2\overline{G_5^2}\beta\frac{\partial^3\phi_{y2}}{\partial Y\partial X^2}-2\overline{l_0}^2\overline{G_5^2}\frac{\partial^3\phi_{x2}}{\partial X^3}+2\overline{l_0}^2\overline{G_3^2}\frac{\partial^5\phi_{x2}}{\partial X^5}\\
&+4\overline{l_0}^2\overline{G_3^2}\beta^3\frac{\partial^5\phi_{y2}}{\partial Y^3\partial X^2}+2\overline{l_0}^2\overline{G_3^2}\beta^5\frac{\partial^5\phi_{y2}}{\partial Y^5}+2\overline{l_0}^2\overline{G_3^2}\beta\frac{\partial^5\phi_{y2}}{\partial Y\partial X^4}\\
&+4\overline{l_0}^2\overline{G_3^2}\beta^2\frac{\partial^5\phi_{x2}}{\partial Y^2\partial X^3}-6\overline{l_0}^2\overline{G_2^2}\alpha\beta^4\frac{\partial^6W_2}{\partial Y^4\partial X^2}+2\overline{l_0}^2\overline{G_0^2}\alpha\beta^4\frac{\partial^4W_2}{\partial Y^4}\\
&+\frac{16}{15}\overline{l_0}^2\overline{G_0^2}\alpha\beta^2\frac{\partial^4W_2}{\partial Y^2\partial X^2}+2\overline{l_0}^2\overline{G_3^2}\beta^4\frac{\partial^5\phi_{x2}}{\partial Y^4\partial X}-6\overline{l_0}^2\overline{G_2^2}\alpha\beta^2\frac{\partial^6W_2}{\partial Y^2\partial X^4}\\
&-2\overline{l_0}^2\overline{G_2^2}\alpha\beta^6\frac{\partial^6W_2}{\partial Y^6}+4\overline{l_0}^2\overline{G_0^2}\alpha\beta^2\frac{\partial^4W_2}{\partial Y^2\partial X^2}+\frac{8}{15}\overline{l_0}^2\overline{G_0^2}\alpha\beta^4\frac{\partial^4W_2}{\partial Y^4}\\
&-2\overline{l_0}^2\overline{G_5^2}\beta^3\frac{\partial^3\phi_{y2}}{\partial Y^3}+2\overline{l_0}^2\overline{G_0^2}\alpha\frac{\partial^4W_2}{\partial X^4}-2\overline{l_0}^2\overline{G_2^2}\alpha\frac{\partial^6W_2}{\partial X^6}+\frac{8}{15}\overline{l_1}^2\overline{G_0^2}\alpha\frac{\partial^4W_2}{\partial X^4}\\
&-\frac{4}{5}\overline{l_1}^2\overline{G_2^2}\alpha\frac{\partial^6W_2}{\partial X^6}-\frac{2}{5}\overline{l_1}^2\overline{G_7^2}\beta^2\frac{\partial^3\phi_{x2}}{\partial Y^2\partial X}+\frac{4}{5}\overline{l_1}^2\overline{G_3^2}\beta^4\frac{\partial^5\phi_{x2}}{\partial Y^4\partial X}\\
&+\frac{8}{5}\overline{l_1}^2\overline{G_3^2}\beta^2\frac{\partial^5\phi_{x2}}{\partial Y^2\partial X^3}+\frac{8}{5}\overline{l_1}^2\overline{G_3^2}\beta^3\frac{\partial^5\phi_{y2}}{\partial Y^3\partial X^2}-\frac{16}{15}\overline{l_1}^2\overline{G_5^2}\beta^3\frac{\partial^5\phi_{y2}}{\partial Y^3}\\
&-\frac{16}{15}\overline{l_1}^2\overline{G_5^2}\beta\frac{\partial^3\phi_{y2}}{\partial Y\partial X^2}-\frac{16}{15}\overline{l_1}^2\overline{G_5^2}\beta^2\frac{\partial^3\phi_{x2}}{\partial Y^2\partial X}-\frac{2}{5}\overline{l_1}^2\overline{G_9^2}\beta\frac{\partial^3\phi_{y2}}{\partial Y\partial X^2}\\
&+\frac{4}{5}\overline{l_1}^2\overline{G_3^2}\beta\frac{\partial^5\phi_{y2}}{\partial Y\partial X^4}-\frac{2}{5}\overline{l_1}^2\overline{G_7^2}\beta^3\frac{\partial^3\phi_{y2}}{\partial Y^3}-\frac{2}{5}\overline{l_1}^2\overline{G_9^2}\frac{\partial^3\phi_{x2}}{\partial X^3}+\frac{4}{5}\overline{l_1}^2\overline{G_3^2}\frac{\partial^5\phi_{x2}}{\partial X^5}\\
&-\frac{16}{15}\overline{l_1}^2\overline{G_2^2}\frac{\partial^3\phi_{x2}}{\partial X^3}-\frac{4}{5}\overline{l_1}^2\overline{G_2^2}\alpha\beta^6\frac{\partial^6W_2}{\partial Y^6}-\frac{12}{5}\overline{l_1}^2\overline{G_2^2}\alpha\beta^4\frac{\partial^6W_2}{\partial Y^4\partial X^2}\\
&-\frac{12}{5}\overline{l_1}^2\overline{G_2^2}\alpha\beta^2\frac{\partial^6W_2}{\partial Y^2\partial X^4}+\frac{4}{5}\overline{l_1}^2\overline{G_3^2}\beta^5\frac{\partial^5\phi_{y2}}{\partial Y^5}-\frac{1}{4}\overline{l_2}^2\overline{G_5^2}\beta^3\frac{\partial^3\phi_{y2}}{\partial Y^3}+\frac{1}{2}\overline{l_2}^2\overline{G_0^2}\alpha\frac{\partial^4W_2}{\partial X^4}\\
&+\frac{1}{2}\overline{l_2}^2\overline{G_0^2}\alpha\beta^4\frac{\partial^4W_2}{\partial Y^4}+3\overline{l_2}^2\overline{G_0^2}\alpha\beta^2\frac{\partial^4W_2}{\partial Y^2\partial X^2}-\frac{1}{4}\overline{l_2}^2\overline{G_5^2}\frac{\partial^3\phi_{x2}}{\partial X^3}-\frac{3}{4}\overline{l_2}^2\overline{G_5^2}\beta\frac{\partial^3\phi_{y2}}{\partial Y\partial X^2}\\
&-\frac{3}{4}\overline{l_2}^2\overline{G_5^2}\beta^2\frac{\partial^3\phi_{x2}}{\partial Y^2\partial X}+4\overline{A_{66}^2}\alpha\beta^2\frac{\partial^4W_2}{\partial Y^2\partial X^2}+\overline{A_{22}^2}\alpha\beta^4\frac{\partial^4W_2}{\partial Y^4}+2\overline{A_{12}^2}\alpha\beta^2\frac{\partial^4W_2}{\partial Y^2\partial X^2}\\
&+\overline{A_{11}^2}\alpha\frac{\partial^4W_2}{\partial X^4}-\overline{D_{12}^2}\beta\frac{\partial^3\phi_{y2}}{\partial Y\partial X^2}-2\overline{D_{12}^2}\beta^2\frac{\partial^3\phi_{x2}}{\partial Y^2\partial X}-\overline{D_{22}^2}\beta^3\frac{\partial^3\phi_{y2}}{\partial Y^3}-2\overline{D_{66}^2}\beta^2\frac{\partial^3\phi_{x2}}{\partial Y^2\partial X}\\
&-2\overline{D_{66}^2}\beta\frac{\partial^3\phi_{y2}}{\partial Y\partial X^2}-\overline{D_{11}^2}\frac{\partial^3\phi_{x2}}{\partial X^3}+\overline{I_3^2}\frac{\partial^3\phi_{x2}}{\partial\tau^2\partial X}-\overline{I_2^2}\alpha\beta^2\frac{\partial^4W_2}{\partial\tau^2\partial Y^2}-\overline{I_2^2}\alpha\frac{\partial^4W_2}{\partial\tau^2\partial X^2}\\
&+\overline{I_0^2}\alpha\frac{\partial^2W_2}{\partial\tau^2}+\overline{I_3^2}\beta\frac{\partial^3\phi_{y2}}{\partial\tau^2\partial Y}-\alpha\beta^2k_Gk_{Gx}^*\frac{\partial^2W_2}{\partial Y^2}+\alpha\beta^2k_Gk_{Gx}^*\frac{\partial^2W_1}{\partial Y^2}-\alpha k_{Gx}^*\frac{\partial^2W_2}{\partial X^2}\\
&+\alpha k_{Gx}^*\frac{\partial^2W_1}{\partial X^2}+C_d^*\frac{\partial W_2}{\partial\tau}-C_d^*\frac{\partial W_1}{\partial\tau}+\alpha k_2k_{w12}^*W-\alpha k_{w12}^*W_1+\alpha k_{w12}^*W_2\\
&-\frac{3}{2}\alpha h^*\overline{P_1}\frac{\partial^2\varphi}{\partial X^2}-\frac{3}{2}\alpha\beta^2h^*\overline{P_1e_{32}}\frac{\partial^2\varphi}{\partial Y^2}=0,
\end{aligned}
\tag{24d}
$$

$\delta\phi_{x2} =$

$$
\begin{aligned}
&2\overline{l_0}^2\overline{G_4^1}\frac{\partial^4\phi_{x2}}{\partial X^4}-2\overline{l_0}^2\overline{G_6^2}\frac{\partial^2\phi_{x2}}{\partial X^2}-2\overline{l_0}^2\overline{G_3^2}\alpha\frac{\partial^3W_2}{\partial X^3}-2\overline{l_0}^2\overline{G_6^2}\beta\frac{\partial^2\phi_{y2}}{\partial Y\partial X}+2\overline{l_0}^2\overline{G_4^2}\beta^3\frac{\partial^4\phi_{y2}}{\partial Y^3\partial X}\\
&+2\overline{l_0}^2\overline{G_5^2}\alpha\frac{\partial W_2}{\partial X^3}+2\overline{l_0}^2\overline{G_4^2}\beta\frac{\partial^4\phi_{y2}}{\partial Y\partial X^3}+2\overline{l_0}^2\overline{G_4^2}\beta^2\frac{\partial^4\phi_{x2}}{\partial Y^2\partial X^2}-4\overline{l_0}^2\overline{G_3^2}\beta^2\alpha\frac{\partial^3W_2}{\partial Y^2\partial X^3}\\
&-2\overline{l_0}^2\overline{G_3^2}\beta^4\alpha\frac{\partial^3W_2}{\partial Y^4\partial X}+2\overline{l_0}^2\overline{G_5^2}\beta^2\alpha\frac{\partial^3W_2}{\partial Y^2\partial X}-\frac{1}{8}\overline{l_1}^2\overline{G_6^2}\frac{\partial^2\phi_{x2}}{\partial X^2}-\frac{4}{5}\overline{l_1}^2\overline{G_7^2}\frac{\partial^2\phi_{x2}}{\partial X^2}\\
&+\frac{4}{5}\overline{l_1}^2\overline{G_4^2}\frac{\partial^4\phi_{x2}}{\partial X^4}-\frac{32}{15}\overline{l_1}^2\overline{G_6^2}\frac{\partial^2\phi_{x2}}{\partial X^2}+\frac{16}{15}\overline{l_1}^2\overline{G_5^2}\alpha\frac{\partial^3W_2}{\partial X^3}+\frac{4}{3}\overline{l_1}^2\overline{G_4^2}\beta^2\frac{\partial^4\phi_{x2}}{\partial X^4}\\
&-\frac{4}{3}\overline{l_1}^2\overline{G_6^2}\beta^2\frac{\partial^2\phi_{x2}}{\partial Y^2}+\frac{8}{15}\overline{l_1}^2\overline{G_4^2}\beta^4\frac{\partial^4\phi_{x2}}{\partial Y^4}-\frac{4}{15}\overline{l_1}^2\overline{G_7^2}\beta^2\frac{\partial^2\phi_{x2}}{\partial Y^2}+\frac{2}{5}\overline{l_1}^2\overline{G_9^2}\alpha\frac{\partial^3W_2}{\partial X^3}\\
&-\frac{4}{5}\overline{l_1}^2\overline{G_3^2}\alpha\frac{\partial^3W_2}{\partial X^5}+\frac{8}{15}\overline{l_1}^2\overline{G_8^2}\phi_{x2}+\frac{4}{15}\overline{l_1}^2\overline{G_4^2}\beta\frac{\partial^4\phi_{x2}}{\partial Y\partial X^3}-\frac{4}{5}\overline{l_1}^2\overline{G_6^2}\beta\frac{\partial^2\phi_{y2}}{\partial Y\partial X}\\
&+\frac{4}{15}\overline{l_1}^2\overline{G_4^2}\beta^3\frac{\partial^4\phi_{y2}}{\partial Y^3\partial X}-\frac{8}{15}\overline{l_1}^2\overline{G_7^2}\beta\frac{\partial^2\phi_{y2}}{\partial Y\partial X}-\frac{8}{5}\overline{l_1}^2\overline{G_3^2}\beta^2\alpha\frac{\partial^3W_2}{\partial Y^2\partial X^3}\\
&+\frac{16}{15}\overline{l_1}^2\overline{G_5^2}\beta^2\alpha\frac{\partial^3W_2}{\partial Y^2\partial X}+\frac{2}{5}\overline{l_1}^2\overline{G_7^2}\beta^2\alpha\frac{\partial^3W_2}{\partial Y^2\partial X}-\frac{4}{5}\overline{l_1}^2\overline{G_3^2}\beta^4\alpha\frac{\partial^3W_2}{\partial Y^4\partial X}-\overline{l_2}^2\overline{G_6^2}\beta^2\frac{\partial^2\phi_{x2}}{\partial Y^2}\\
&-\frac{1}{8}\overline{l_2}^2\overline{G_4^2}\beta^3\frac{\partial^4\phi_{y2}}{\partial Y^3\partial X}+\frac{5}{8}\overline{l_2}^2\overline{G_6^2}\beta\frac{\partial^2\phi_{y2}}{\partial Y\partial X}+\frac{1}{4}\overline{l_2}^2\overline{G_7^2}\beta\frac{\partial^2\phi_{y2}}{\partial Y\partial X}-\frac{1}{4}\overline{l_2}^2\overline{G_7^2}\beta^2\frac{\partial^2\phi_{x2}}{\partial Y^2}\\
&+\frac{1}{8}\overline{l_2}^2\overline{G_4^2}\beta^2\frac{\partial^4\phi_{x2}}{\partial Y^2\partial X^2}+\frac{1}{8}\overline{l_2}^2\overline{G_4^2}\beta^4\frac{\partial^4\phi_{x2}}{\partial Y^4}+\frac{1}{4}\overline{l_2}^2\overline{G_5^2}\alpha\frac{\partial^3W_2}{\partial X^3}-\frac{1}{8}\overline{l_2}^2\overline{G_4^2}\beta\frac{\partial^4\phi_{y2}}{\partial Y\partial X^3}\\
&+\frac{1}{8}\overline{l_2}^2\overline{G_8^2}\phi_{x2}+\frac{3}{4}\overline{l_2}^2\overline{G_5^2}\beta^2\alpha\frac{\partial^3W_2}{\partial Y^2\partial X}+\overline{C_{55}^2}\phi_{x2}-\overline{B_{66}^2}\beta^2\frac{\partial^2\phi_{x2}}{\partial Y^2}-\overline{B_{66}^2}\beta\frac{\partial^2\phi_{y2}}{\partial Y\partial X}\\
&-\overline{B_{12}^2}\beta\frac{\partial^2\phi_{y2}}{\partial Y\partial X}-\overline{B_{12}^2}\frac{\partial^2\phi_{x2}}{\partial X^2}+\overline{D_{11}^2}\alpha\frac{\partial^3W_2}{\partial X^3}+2\overline{D_{12}^2}\beta^2\alpha\frac{\partial^3W_2}{\partial Y^2\partial X}+2\overline{D_{66}^2}\beta^2\alpha\frac{\partial^3W_2}{\partial Y^2\partial X}\\
&-\overline{I_3^2}\alpha\frac{\partial^3W_2}{\partial\tau^2\partial X}+\overline{I_4^2}\frac{\partial^2\phi_{x2}}{\partial\tau^2}+\frac{3}{2}\alpha\overline{P_2e_{15}}\frac{\partial\varphi}{\partial X}-\frac{3}{2}\alpha h^*\overline{P_5}\frac{\partial\varphi}{\partial X}=0,
\end{aligned}
\tag{24e}
$$

$\delta\phi_{y2} =$

$$
\begin{aligned}
&2\overline{l_0}^2\overline{G_4^2}\beta\frac{\partial^4\phi_{x2}}{\partial Y\partial X^3}-2\overline{l_0}^2\overline{G_6^2}\beta^2\frac{\partial^2\phi_{y2}}{\partial Y^2}+2\overline{l_0}^2\overline{G_4^2}\beta^4\frac{\partial^4\phi_{y2}}{\partial Y^4}+2\overline{l_0}^2\overline{G_4^2}\beta^2\frac{\partial^4\phi_{y2}}{\partial Y^2\partial X^2}\\
&+2\overline{l_0}^2\overline{G_4^2}\beta^3\frac{\partial^4\phi_{x2}}{\partial Y^3\partial X}-2\overline{l_0}^2\overline{G_6^2}\beta\frac{\partial^2\phi_{x2}}{\partial Y\partial X}+2\overline{l_0}^2\overline{G_5^2}\alpha\beta^3\frac{\partial^3W_2}{\partial Y^3}+2\overline{l_0}^2\overline{G_5^2}\alpha\beta\frac{\partial^3W_2}{\partial Y\partial X^2}\\
&-2\overline{l_0}^2\overline{G_3^2}\alpha\beta^5\frac{\partial^3W_2}{\partial Y^5}-2\overline{l_0}^2\overline{G_3^2}\alpha\beta\frac{\partial^3W_2}{\partial Y\partial X^4}-4\overline{l_0}^2\overline{G_3^2}\alpha\beta^3\frac{\partial^3W_2}{\partial Y^3\partial X^2}+\frac{8}{15}\overline{l_1}^2\overline{G_4^2}\frac{\partial^4\phi_{y2}}{\partial X^4}\\
&-\frac{4}{3}\overline{l_1}^2\overline{G_6^2}\frac{\partial^2\phi_{y2}}{\partial X^2}-\frac{4}{15}\overline{l_1}^2\overline{G_7^2}\frac{\partial^2\phi_{y2}}{\partial X^2}+\frac{8}{15}\overline{l_1}^2\overline{G_8^2}\phi_{y2}+\frac{4}{15}\overline{l_1}^2\overline{G_4^2}\beta\frac{\partial^4\phi_{x2}}{\partial Y\partial X^3}\\
&+\frac{4}{3}\overline{l_1}^2\overline{G_4^2}\beta^2\frac{\partial^4\phi_{y2}}{\partial Y^2\partial X^2}+\frac{4}{5}\overline{l_1}^2\overline{G_4^2}\beta^4\frac{\partial^4\phi_{y2}}{\partial Y^4}-\frac{4}{5}\overline{l_1}^2\overline{G_7^2}\beta^2\frac{\partial^2\phi_{y2}}{\partial Y^2}-\frac{8}{15}\overline{l_1}^2\overline{G_7^2}\beta\frac{\partial^2\phi_{x2}}{\partial Y\partial X}\\
&-\frac{4}{5}\overline{l_1}^2\overline{G_6^2}\beta\frac{\partial^2\phi_{x2}}{\partial Y\partial X}-\frac{32}{15}\overline{l_1}^2\overline{G_6^2}\beta^2\frac{\partial^2\phi_{y2}}{\partial Y^2}-\frac{4}{5}\overline{l_1}^2\overline{G_3^2}\alpha\beta\frac{\partial^5W_2}{\partial Y\partial X^4}+\frac{2}{5}\overline{l_1}^2\overline{G_7^2}\alpha\beta^3\frac{\partial^3W_2}{\partial Y^3}\\
&+\frac{4}{15}\overline{l_1}^2\overline{G_4^2}\alpha\beta^3\frac{\partial^4\phi_{x2}}{\partial Y^3\partial X}-\frac{4}{5}\overline{l_1}^2\overline{G_3^2}\alpha\beta^5\frac{\partial^5W_2}{\partial Y^5}+\frac{16}{15}\overline{l_1}^2\overline{G_5^2}\alpha\beta^3\frac{\partial^3W_2}{\partial Y^3}\\
&-\frac{8}{5}\overline{l_1}^2\overline{G_3^2}\alpha\beta^3\frac{\partial^5W_2}{\partial Y^3\partial X^2}+\frac{16}{15}\overline{l_1}^2\overline{G_5^2}\alpha\beta\frac{\partial^3W_2}{\partial Y\partial X^2}+\frac{2}{5}\overline{l_1}^2\overline{G_9^2}\alpha\beta\frac{\partial^3W_2}{\partial Y\partial X^2}\\
&+\frac{3}{4}\overline{l_2}^2\overline{G_5^2}\alpha\beta\frac{\partial^3W_2}{\partial Y\partial X^2}+\frac{1}{4}\overline{l_2}^2\overline{G_5^2}\alpha\beta^3\frac{\partial^3W_2}{\partial Y^3}-\frac{1}{8}\overline{l_2}^2\overline{G_6^2}\beta^2\frac{\partial^2\phi_{y2}}{\partial Y^2}+\frac{1}{8}\overline{l_2}^2\overline{G_4^2}\frac{\partial^4\phi_{y2}}{\partial X^4}\\
&-\overline{l_2}^2\overline{G_6^2}\frac{\partial^2\phi_{y2}}{\partial X^2}-\frac{1}{4}\overline{l_2}^2\overline{G_7^2}\frac{\partial^2\phi_{y2}}{\partial X^2}+\frac{1}{8}\overline{l_2}^2\overline{G_8^2}\phi_{y2}+\frac{1}{4}\overline{l_2}^2\overline{G_7^2}\beta\frac{\partial^2\phi_{x2}}{\partial Y\partial X}+\frac{5}{8}\overline{l_2}^2\overline{G_6^2}\beta\frac{\partial^2\phi_{y2}}{\partial Y\partial X}\\
&-\frac{1}{8}\overline{l_2}^2\overline{G_4^2}\beta^3\frac{\partial^4\phi_{x2}}{\partial Y^3\partial X}-\frac{1}{8}\overline{l_2}^2\overline{G_4^2}\beta\frac{\partial^4\phi_{x2}}{\partial Y\partial X^3}+\frac{1}{8}\overline{l_2}^2\overline{G_4^2}\beta^2\frac{\partial^4\phi_{y2}}{\partial Y^2\partial X^2}+\overline{C_{44}^2}\phi_{y2}\\
&-\overline{B_{66}^2}\beta\frac{\partial^2\phi_{x2}}{\partial Y\partial X}-\overline{B_{12}^2}\beta\frac{\partial^2\phi_{x2}}{\partial Y\partial X}-\overline{B_{22}^2}\beta^2\frac{\partial^2\phi_{y2}}{\partial Y^2}-\overline{B_{66}^2}\frac{\partial^2\phi_{y2}}{\partial X^2}+\overline{D_{22}^2}\alpha\beta^3\frac{\partial^3W_2}{\partial Y^3}\\
&+2\overline{D_{66}^2}\alpha\beta\frac{\partial^3W_2}{\partial Y\partial X^2}+\overline{D_{12}^2}\alpha\beta\frac{\partial^3W_2}{\partial Y\partial X^2}+\overline{I_4^2}\frac{\partial^2\phi_{y2}}{\partial\tau^2}-\overline{I_3^2}\alpha\beta\frac{\partial^3W_2}{\partial\tau^2\partial Y}+\frac{3}{2}\alpha\beta\overline{P_2e_{24}}\frac{\partial\varphi}{\partial Y}\\
&-\frac{3}{2}\alpha\beta h^*\overline{P_5e_{32}}\frac{\partial\varphi}{\partial Y}=0,
\end{aligned}
\tag{24f}
$$

$\delta\varphi =$

$$
\begin{aligned}
&2\alpha\overline{P_4}\frac{\partial^2}{\partial X^2}\varphi+2\alpha\beta^2\overline{P_{22}}\frac{\partial^2\varphi}{\partial Y^2}-2\frac{h^{*2}}{\alpha}\overline{P_{33}}\varphi-\frac{3}{2}\alpha^2h^*\overline{P_1}\frac{\partial^2w}{\partial X^2}\\
&-\frac{3}{2}\alpha^2\beta^2h^*\overline{P_1e_{32}}\frac{\partial^2w}{\partial Y^2}-\frac{3}{2}\alpha\overline{P_2e_{15}}\frac{\partial\phi_x}{\partial X}+\frac{3}{2}\alpha h^*\overline{P_5}\frac{\partial\phi_x}{\partial X}\\
&+\frac{3}{2}\alpha\beta h^*\overline{P_5e_{32}}\frac{\partial\phi_y}{\partial Y}-\frac{3}{2}\alpha\beta\overline{P_2e_{24}}\frac{\partial\phi_y}{\partial Y}=0.
\end{aligned}
\tag{24g}
$$

8. Solution procedure

To solve equations of motion for the simply-supported sandwich microplates, the Navier's type solution is chosen. According to this approach, the displacements are considered as functions which satisfy at least the various geometric boundary conditions. Thus, the displacement variables of sandwich plates can be written in the following forms (Mohammadimehr *et al.* 2016d)

$$
\begin{aligned}
w_{1,2}(x,y,t)&=\sum_{n=1}^{N}\sum_{m=1}^{M}W_{1,2mn}\sin(m\pi X)\sin(n\pi Y)e^{i\Omega_{mn}\tau},\\
\phi_{x1,2}(x,y,t)&=\sum_{n=1}^{N}\sum_{m=1}^{M}P_{1,2mn}\cos(m\pi X)\sin(n\pi Y)e^{i\Omega_{mn}\tau},\\
\phi_{y1,2}(x,y,t)&=\sum_{n=1}^{N}\sum_{m=1}^{M}Q_{1,2mn}\sin(m\pi X)\cos(n\pi Y)e^{i\Omega_{mn}\tau},\\
\varphi(x,y,t)&=\sum_{n=1}^{N}\sum_{m=1}^{M}\varphi_{mn}\sin(m\pi X)\sin(n\pi Y)e^{i\Omega_{mn}\tau},
\end{aligned}
\tag{25}
$$

where *m* and *n* indicate half axial and transverse wave numbers, respectively. Also, Ω_{mn} is the dimensionless natural frequency.

Substituting Eq. (25) into Eq. (24) leads to final relations as matrix form

$$
\underbrace{\left[M(i\Omega)^2+C(i\Omega)+K\right]}_{Coefficients\ matrix}\{W_{1mn}\quad P_{1mn}\quad Q_{1mn}\quad W_{2mn}\quad P_{2mn}\quad Q_{2mn}\quad \varphi_{mn}\}^T=\{0\}.
\tag{26}
$$

The elements of matrices *M*, *C* and *K* in Eqs. (26) are

Table 1 Mechanical properties of core and facesheets for sandwich microplate

Material	E_{11} (TPa)	E_{11}	G_{12}	ρ (Kg/m^3)	v
CNT (Zhu *et al.* 2012)	5.6466	7.08	1.9445	1750	0.17
BNNT (Ghorbanpour Arani and Amir 2013)	1.8	1.8	0.7895	2300	0.14
PMPV (core of SP1 and SP2) (Mohammadimehr *et al.* 2016a)	2.1×10^{-3}	2.1×10^{-3}	$E_{11}/2(1+v)$	1150	0.34
PMMA (Facesheet matrix of SP1) (Natarajan *et al.* 2014)	2.5×10^{-3}	2.5×10^{-3}	$E_{11}/2(1+v)$	1150	0.34
PVDF (Facesheet matrix of SP2) (Mohammadimehr *et al.* 2016c)	2×10^{-3}	2×10^{-3}	$E_{11}/2(1+v)$	1780	0.3

Table 2 Electrical Properties of PVDF and BNNT (Pietrzakowski 2008, Ghorbanpour Arani *et al.* 2012)

Material	e_{31} (C/m^2)	e_{32}	e_{24}	e_{15}	$\frac{\epsilon_{11}}{\epsilon_0^*}(F/m)$	$\frac{\epsilon_{22}}{\epsilon_0^*}$	$\frac{\epsilon_{33}}{\epsilon_0^*}$
PVDF	-0.13	-0.145	-0.009	-0.135	12.5	11.98	11.98
BNNT	0	0	0	0	1250	1250	1250

$\epsilon_0^* = 8.854185\times10^{-12}$

expressed in Appendix C with details.

By Substituting Eq. (25) into Eqs. (24a)-(24g), the partial differential equations are converted to algebraic equations as matrix form in Eq. (26). In order to obtain dimensionless natural frequencies from Eq. (26) must be determined eigenvalues of coefficients matrix. By calculating determinant of coefficients matrix, characteristic natural frequency equation is obtained in which smallest root of this equation is the dimensionless fundamental natural frequency.

9. Numerical results and discussion

In this section, the effects of various parameters such as geometric, mechanical, elastic foundation and other parameters, on the natural frequencies of double-bonded sandwich micro-plates are discussed in details. The values of materials properties are defined in Tables 1 and 2 for SP1 and SP2, respectively. According to Ghorbanpour Arani and Haghparast (2015), h/l_i=3 is assumed and the other geometrical properties of sandwich microplates are considered as h=4 μm, b/h=10 and a/b=1. Also, the efficiency parameters are considered by Mohammadimehr *et al.* (2015) for $V_{NT}^* = 0.17$ which are equal to η_1=0.142, η_2=1.62 and η_3=1.138. The efficiency parameters for CNTs are obtained by molecular dynamics simulations (Han and Elliott 2007). Since these values have not yet been calculated for BNNTs, based on Mohammadimehr *et al.* (2016a), we had to consider these values for BNNTs. Mohammadimehr *et al.* 2016a in their paper assumed the values for BNNTs and there is not any value for BNNTs in the literature based on molecular dynamics. Except for those mentioned, all figures are plotted for the following conditions:

CT, UU distribution of nanotubes, $k_{w12}^* = 5000$, k_1=k_2=1, $k_{Gx}^* = k_{Gy}^* = C_d^* = 0$ and t^*=2.

In order to evaluate the reliability of the present work, the dimensionless natural frequencies are compared with previous works in the literature. Table 3 exhibits comparison between dimensionless natural frequencies of a simply supported isotropic plate at the different temperatures. As can be seen, the results of present work show excellent agreement with the reported results by Aghababaei and Reddy (2009) and Hosseini-Hashemi *et al.* (2015). Also, comparison between dimensionless natural frequencies of a simply supported square sandwich plate with a homogeneous core and CNT reinforced composite

Table 3 Comparison between dimensionless natural frequencies of a simply supported isotropic plate (E=30 GPa, ρ=1 kg/m^3, v=3, $D=Eh^3/12(1-v^2)$ and $\varpi = \omega a^2\sqrt{\rho h/D}$)

a/b	h/a	Author(s)	Theory	Frequency	Error (%)
1.0	0.10	Aghababaei and Reddy (2009)	HSDT	19.1678	0.532
		Hosseini-Hashemi *et al.* (2015)	HSDT	19.0653	0.003
		Present	SSDT	19.0659	-
	0.05	Aghababaei and Reddy (2009)	HSDT	19.6695	0.544
		Hosseini-Hashemiet *et al.* (2015)	HSDT	19.5625	0
		Present	SSDT	19.5625	-
0.5	0.10	Aghababaei and Reddy (2009)	HSDT	12.1157	0.396
		Hosseini-Hashemiet *et al.* (2015)	HSDT	12.0675	.002
		Present	SSDT	12.0677	-
	0.05	Aghababaei and Reddy (2009)	HSDT	12.3445	0.624
		Hosseini-Hashemiet *et al.* (2015)	HSDT	12.2675	0
		Present work	SSDT	12.2675	-

Table 4 Comparison between dimensionless natural frequencies of a simply supported square sandwich platewith a homogeneous core and UD type of CNT reinforced composite facesheets (T=300, h_c/h_f=2, $V_{CNT}^* = .17$ and $\varpi = \omega\frac{a^2}{h}\sqrt{\rho_c/E_c}$)

a/b	Author(s)	Theory	Frequency	Error (%)
5	Natarajan *et al.* (2014)	TSDT	4.3199	7.750
	Present work	SSDT	4.6547	
10	Natarajan *et al.* (2014)	TSDT	4.6655	6.109

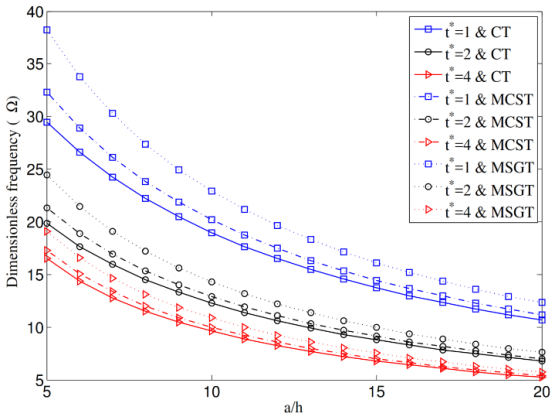

Fig. 3 The dimensionless first natural frequency of double bonded sandwich microplates versus length to thickness ratio for different core to facesheet thickness ratio ($t^*=h_c/h_f$) and various theories

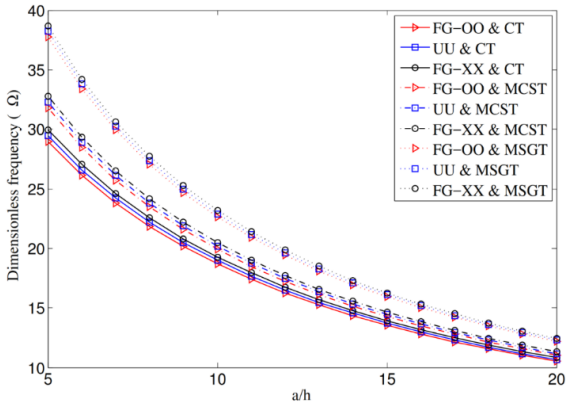

Fig. 4 The dimensionless frequency of double bonded sandwich microplates versus length to thickness ratio for symmetric distributions of nanotubes and various theories ($t^*=1$)

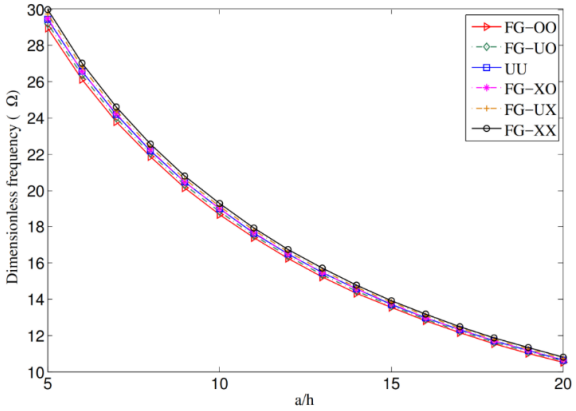

Fig. 5 The dimensionless frequency of double-bonded sandwich microplates versus length to thickness ratio for various distributions of nanotubes ($t^*=1$)

facesheets are presented in Table 4. Natarajan *et al.* (2014) suggest various theories for displacement field. The results of this research for SSDT are compared with the TSDT results obtained by Natarajan *et al.* (2014) that there is an acceptable agreement between them.

Fig. 3 illustrates the dimensionless natural frequency of double-bonded sandwich microplates versus length to thickness ratio for different core to facesheet thickness ratio ($t^*=h_c/h_f$) and various theories such as classical theory (CT), modified couple stress theory (MCST), and modified strain gradient theory (MSGT). Also, in Eq. (21), l_0, l_1, and l_2 denote three additional independent material length scale parameters associated with the dilatation gradients, deviatoric stretch gradients and symmetric rotation gradients, respectively. If the parameters l_0 and l_1 should be equal to zero, then the modified strain gradient theory (MSGT) in Eq. (21) is converted to the modified couple stress theory (MCST). Also, if three material length scale parameters should be equal to zero, then the classical theory is obtained. Thus, there is a discrepancy between the results of different theories including MSGT(l_0, l_1, $l_2\neq0$, MCST ($l_0=l_1=0$), and CT ($l_0=l_1=l_2=0$).

As can be observed in this figure, increasing length to thickness ratio of sandwich microplate leads to decrease dimensionless natural frequencies. Due to core is softer than facesheets, increasing t^* cause to decrease stiffness of sandwich microplates. With considering three material length scale parameters, the stiffness of sandwich micro-plates increases. Thus, MSGT gives higher natural frequencies in comparison with MCST and CT.

At nano scales, the stress field at a reference point x in an elastic medium is considered to depend on not only the strain at that point but also the strains at all other points in the domain while based on local elasticity theory (or classical theory), the stress field at a reference point x in an elastic medium is only depend on the strain at that point. Therefore, the use of modified strain gradient theory (MSGT) and modified coupled stress theory (MCST) at micro scale and nonlocal Eringen at nano scale were suggested which are consider the size effects. In this work, the geometrical parameters of sandwich plates are at micro scale. Thus, MSGT is used in the present work. In Fig. 3, the dimensionless natural frequency of nancomposite plate obtained by MSGT is higher than that of for CT and MCST. This means that the nanocomposite plate becomes stiffer with considering MSGT. On the other hands, the size effect at micro scale leads to increase the stiffness of nanocomposite plate as well as dimensionless natural frequency.

Fig. 4 displays the dimensionless first natural frequency of double-bonded sandwich microplates versus length to thickness ratio for symmetric distributions of nanotubes and various theories. It can be found that FG-XX distribution gives higher dimensionless natural frequencies rather than UU and FG-OO distributions, respectively. Generally, the employing various distributions of nanotubes are effective manner to achieve greater stiffness.

Fig. 5 shows the dimensionless natural frequency of double-bonded sandwich microplates versus length to thickness ratio for symmetric and un-symmetric distributions of nanotubes. It is concluded that the highest and lowest natural frequency belongs to the FG-XX and FG-OO, respectively. As one of the remarkable results of this figure, it can be noted that the dimensionless frequencies for the UU type are similar to the FG-XO type.

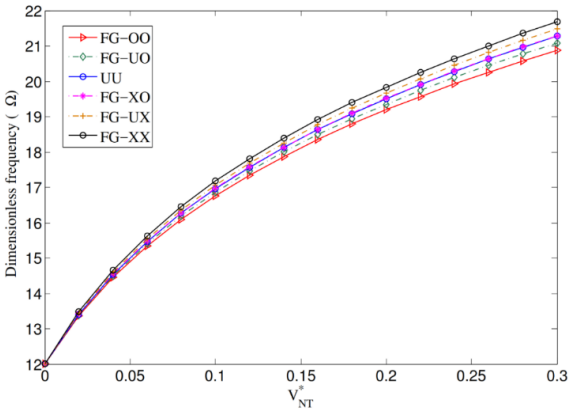

Fig 6 The effect of volume fraction of nanotubeson the dimensionless frequency of double-bonded sandwich microplates for various distributions of nanotubes(t^*=1)

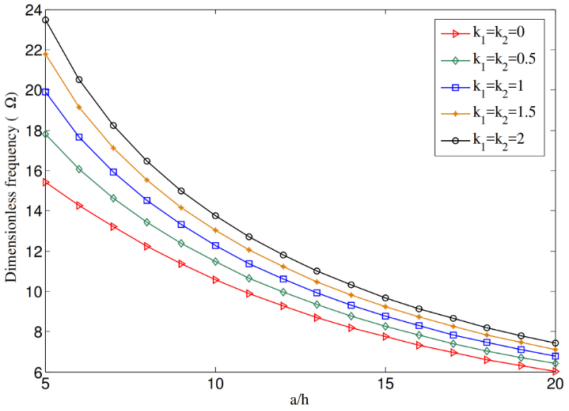

Fig. 8 The dimensionless natural frequency of double-bonded sandwich microplates versus aspect ratio (length to thickness ratio) for various spring modulus ratio (k_1 and k_2)

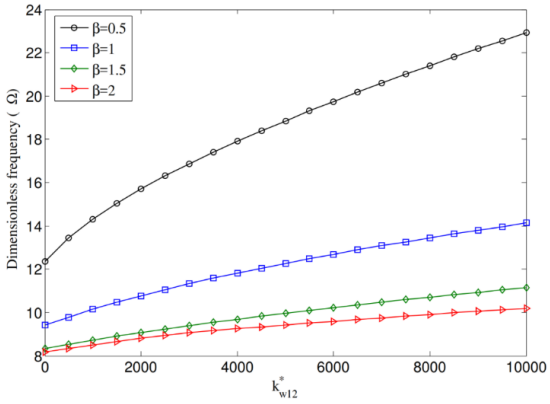

Fig. 7 The effect of dimensionless Winkler constant on the dimensionless frequency of double bonded sandwich microplates in different side ratio

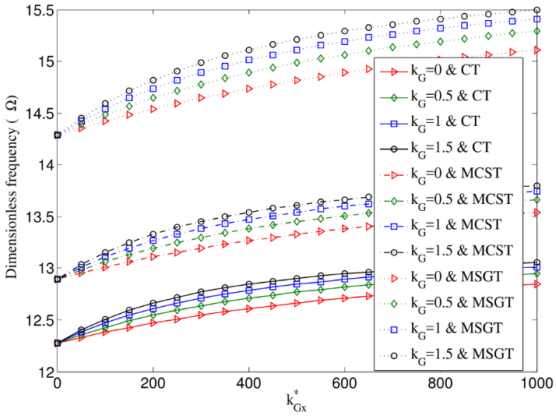

Fig. 9 The effect of shear layer constant along *x* direction on the dimensionless frequency of double bonded sandwich microplates for different shear layer constants ratio (k_G) and various theories

Because of the stiffness of obtained sandwich plates by two distributions is equal.

Fig. 6 presents the effect of volume fraction of nanotubes on the dimensionless frequency of double-bonded sandwich microplates for symmetric and un-symmetric distributions of nanotubes. According to this figure, increasing the volume fraction of nanotubes leads to increase stiffness of sandwich microplates and therefore, natural frequency increases. Only by adding 30% of nanotubes in the polymer matrix of facesheets, the natural frequency can be grown up to 75%, approximately. It proves the irrefutable role of nanotubes in reinforcement of polymer matrix.

Fig. 7 presents the effect of dimensionless Winkler constant on the dimensionless frequency of double-bonded sandwich microplates in different side ratio (length to width). The spring modulus of the elastic foundation increases stiffness of system and cause to stable it. Also, when the side ratio increases, the values of dimensionless frequency decrease.

The dimensionless frequency of double-bonded sandwich microplates versus aspect ratio (length to thickness ratio) for various spring modulus ratio (k_1 and k_2) is illustrated in Fig. 8. It's obvious that increasing spring modulus ratio leads to increase dimensionless frequency. The interesting point is that the effect of this ratio on increasing dimensionless frequency is noticeable.

Fig. 9 depicts the effect of shear layer constant along *x* direction on the dimensionless frequency of double-bonded sandwich microplates for different shear layer constants ratio ($k_G = k^*_{Gy} / k^*_{Gx}$) and various theories. In order to enhance the stability of systems, one of the options can be adding shear layers. Increasing shear layer constant along *x* direction leads to improve natural frequency. Also, adding shear layer along *y* direction and reinforcement it, can be further increase natural frequency. Also, the dimensionless frequencies of MSGT are larger than MCST and CT due to consider three material lengths scale parameters in MSGT.

Fig. 10 shows the effect of dimensionless damping coefficient on the dimensionless frequency of double-bonded sandwich microplates for various theories. As the damping coefficient increases, the natural frequency is reduced until it reaches to the zero natural frequency. At this time, the structure becomes unstable which knowing this problem is very useful optimum design and control of similar systems such as micro-electro-mechanical and nano-electro-mechanical devices.

The influence of 2D magnetic fields on the dimensionless

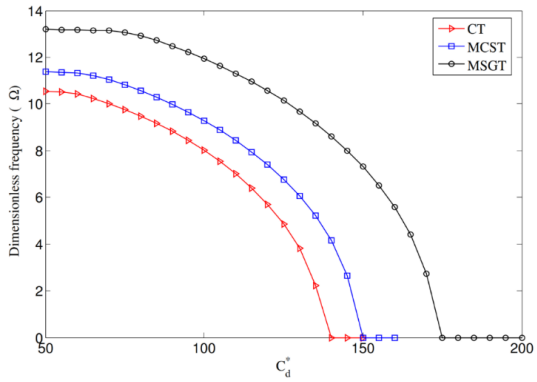

Fig. 10 The effect of dimensionless damping coefficient on the dimensionless frequency of double-bonded sandwich microplates for various theories. ($k_{w12}^* = 0$)

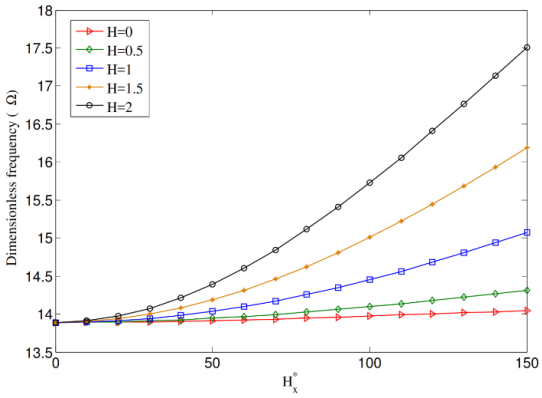

Fig. 11 The influence of 2D magnetic fields on the dimensionless frequency of sandwich microplates with CNT reinforced facesheets for different transverse to longitudinal magnetic field intensity ratio ($H = H_y^* / H_x^*$)

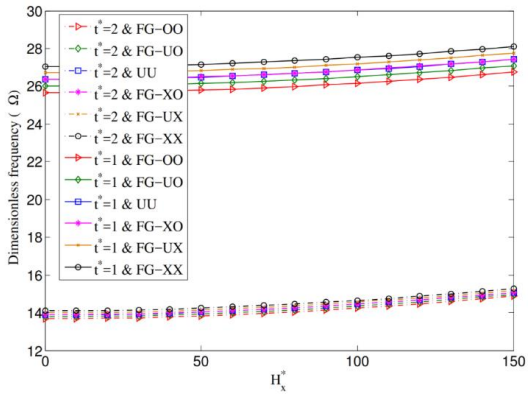

Fig. 12 The influence of 2D magnetic fields on the dimensionless frequency of sandwich microplates with CNT reinforced facesheets for different t^* and various distributions of SWCNT ($\overline{k_{w12}} = 0$)

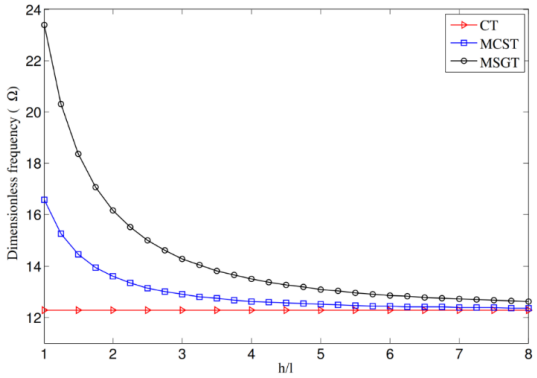

Fig. 13 The effect of material length scale parameter on the dimensionless frequency of double bonded sandwich microplates for various theories

frequency of sandwich microplates with CNT reinforced facesheets for different transverse to longitudinal magnetic field intensity ratio ($H = H_y^* / H_x^*$) is displayed in Fig. 11. As can be observed, applying the longitudinal magnetic field can increase the natural frequencies slightly, while increasing the natural frequencies can be more by adding the transverse magnetic field. It is due to enlarge the created Lorentz forces by 2D magnetic fields where improves the stability of sandwich microplates for CNT reinforced facesheets.

Fig. 12 demonstrates the influence of 2D magnetic fields on the dimensionless frequency of sandwich microplates with CNT reinforced facesheets for different t^* and symmetric and un-symmetric distributions of SWCNT. According to this figure, decreasing the thickness ratio (the core thickness with respect to facesheets thickness) as well as enhancing the intensity of 2D magnetic fields, leads to increase the dimensionless frequency. Also, the slope of curves is almost constant for symmetric and un-symmetric distributions of SWCNT in this figure. Moreover, in lower the thickness ratio, the effects of FG-CNTs on the dimensionless first natural frequency are noticeable.

Fig. 13 presents the effect of material length scale parameter on the dimensionless frequency of double-bonded sandwich microplates for various theories. This figure reveals that the value of dimensionless frequency predicted by MSGT is more sensitive to *h/l* rather than MCST. The effect of material length scale parameter in MSGT and MCST on the dimensionless frequency is negligible for *h/l*≥5 (Mohammadimehr *et al.* 2016d). According to this, the appropriate selection of *h/l* is very important in order to achieve the best results.

A sandwich structure are made of a core and top and bottom facesheets that core is thicker and softer than facesheets. For this reason, it must use a high order theory to consider in-plane and higher order out of plane deformations. Classical plate theory (CPT) considers in-plane and bending deformation while sinusoidal shear deformation plate theory (SSDT) considers in-plane and higher order out of plane deformations with high accuracy. CPT can be obtained by inserting $\psi(z)=0$ in Eq. (3). Therefore, in this research, it can be considered SSDT for all layers of sandwich plate to simplify final relationships. In order to compare the results of CPT and SSDT for core and two facesheets in this work, the dimensionless natural frequency of double-bonded sandwich microplates versus length to thickness ratio is shown Fig. 14. It can be seen, the dimensionless natural frequencies obtained by CPT are higher than SSDT. Moreover, it is evident that the results of

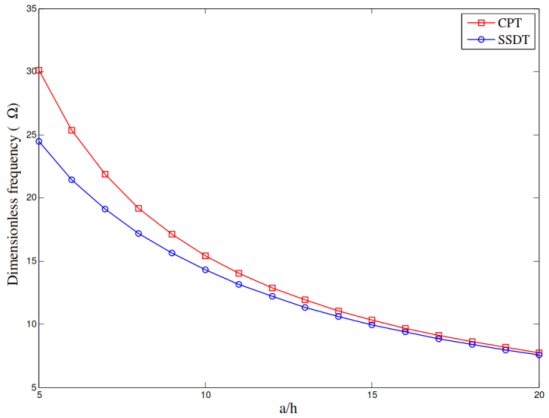

Fig. 14 The dimensionless natural frequency of double-bonded sandwich microplates versus length to thickness ratio for CPT and SSDT

CPT are close to SSDT for higher a/h. It is better that the CPT and SSDT are used for two facesheets and core, respectively, that in this work, we consider SSDT for facesheets and core that these results cover the obtained results by the CPT and SSDT for two facesheets and core, respectively.

10. Conclusions

In this paper, the free vibration of double-bonded sandwich microplates with homogenous core and composite facesheets was investigated under two dimensional magnetic fields and electric field. The extended rule of mixture was employed to obtain structural properties of composite facesheets reinforced by symmetric and un-symmetric distributions of FG-SWCNT and FG-BNNT. Also, the influences of material length scale on the dimensionless frequency of double-bonded sandwich microplates were studied based on modified strain gradient theory (MSGT). Hamilton's principle was utilized to derive the equations of motion and Navier's type solution was used to solve them for all edges simply supported boundary conditions. The results of this work were compared with the existing researches in the literature to confirm the verity of relations and obtained results. The outstanding conclusions of present study are classified as follows:

- Due to facesheets of sandwich microplate are stiffer than core, increasing thickness of core to facesheets ratio leads to decrease the natural frequency.
- Based on MSGT, considering the material length scale parameter causes to increase the dimensionless natural frequency of double-bonded sandwich microplates. Also, the dimensionless natural frequency for MSGT is higher than modified couple stress theory (MCST) and classical theory (CT).
- In each three theories, for FG-XX and FG-OO distributions of nanotubes, highest and lowest dimensionless natural frequency of double-bonded sandwich microplates happens, respectively. Also, the obtained results for uniform distribution (UU) are completely similar to FG-XO.
- Increasing volume fraction of nanotubes in the polymer matrix of facesheets leads to enhance stiffness of sandwich microplates and thus, natural frequency increases. According to the obtained results, the natural frequency can be grown up to 75% by adding 30%of nanotubes, approximately.
- The dimensionless natural frequency of double-bonded sandwich microplates can increase by increasing Winkler and shear layers constants and decreasing damping constant.
- Applying 2D magnetic fields (longitudinal and transverse magnetic fields) in comparison with 1D magnetic field (just longitudinal magnetic field) has more enhance on the stability of sandwich microplates.

The results of present work can be utilized to design micro-electro-mechanical and nano-electro-mechanical devices.

Acknowledgments

The authors would like to thank the referees for their valuable comments. Also, they are thankful to the Iranian Nanotechnology Development Committee for their financial support and the University of Kashan for supporting this work by Grant No. 574602/2.

References

Aghababaei, R, and Reddy, J.N. (2009), "Nonlocal third-order shear deformation plate theory with application to bending and vibration of plates", *J. Sound Vib.*, **326**, 277-289.

Ahn, N. and Lee, K. (2011), "A study on transverse vibration characteristics of a sandwich plate with asymmetrical faces", *Struct. Eng. Mech.*, **40**(4), 501-516.

Arefi, M. (2016), "Buckling analysis of the functionally graded sandwich rectangular plates integrated with piezoelectric layers under bi-axial loads", *J. Sandw. Struct. Mater.*, DOI: https://doi.org/10.1177/1099636216642393.

Daouadji, T.H. and Adim, B. (2017), "Mechanical behavior of FGM sandwich plates using a quasi-3D higher order shear and normal deformation theory", *Struct. Eng. Mech.*, **61**(1), 49-63.

Esawi, A.M.K. and Farag, M.M. (2007), "Carbon nanotube reinforced composites: potential and current challenges", *Mater. Des.*, **28**(9), 2394-2401.

Ghorbanpour Arani, A. and Amir, S. (2013), "Electro-thermal vibration of visco elastically coupled BNNT systems conveying fluid embedded on elastic foundation via strain gradient theory", *Physica B*, **419**, 1-6.

Ghorbanpour Arani, A. and Haghparast, E. (2015), "Size-dependent vibra tion of axially moving viscoelastic microplates based on sinusoidal shear deformation theory", *Int. J. Appl. Mech.*, **9**, 1750026-20.

Ghorbanpour Arani, A., Jamali, M., Ghorbanpour Arani, A.H., Kolahchi, R. and Mosayyebi, M. (2016b), "Electro-magneto wave propagation analysis of viscoelastic sandwich nanoplates considering surface effects", *J. Mech. Eng. Sci.*, **231**(2), 387-403.

Ghorbanpour Arani, A., Shajari, A.R., Amir, S. and Loghman, A. (2012), "Electro-thermo-mechanical nonlinear nonlocal vibration and instability of embedded micro-tube reinforced by BNNT, conveying fluid", *Physica E*, **45**, 109-121.

Ghorbanpour Arani A., Haghparast E. and BabaAkbar Zarei, H.

(2016a), "Vibration of axially moving 3-phase CNTFPC plate resting on orthotropic foundation", *Struct. Eng. Mech.*, **57**(1), 105-126.

Grover, N., Singh, B.N. and Maiti, D.K. (2013), "Analytical and finite element modeling of laminated composite and sandwich plates: An assessment of a new shear deformation theory for free vibration response", *Int. J. Mech. Sci.*, **67**, 89-99.

Han, Y. and Elliott, J. (2007), "Molecular dynamics simulations of the elastic properties of polymer/carbon nanotube composites", *Comput. Mater. Sci.*, **39**, 315-323.

Hosseini-Hashemi, Sh., Kermajani, M. and Nazemnezhad, R. (2015), "An analytical study on the buckling and free vibration of rectangular nanoplates using nonlocal third-order shear deformation plate theory", *Eur. J. Mech. A Solid.*, **51**, 29-43.

Hosseini Hashemi, Sh., Es'haghi, M. and Karimi, M. (2010), "Closed-form vibration analysis of thick annular functionally graded plates with integrated piezoelectric layers", *Int. J. Mech. Sci.*, **52**, 410-428.

Kavalur, P., Jeyaraj, P. and Ravindra Babu, G. (2014), "Static behavior of visco-elastic sandwich plate with nano composite facing under mechanical load", *Procedia Mater. Sci.*, **5**, 1376-1384.

Kheirikhah, M.M., Khalili, S.M.R. and Malekzadeh Fard, K. (2012), "Biaxial buckling analysis of soft-core composite sandwich plates using improved high-order theory", *Eur. J. Mech. A Solid.*, **31**, 54-66.

Kiani, Y. and Eslami, M.R. (2012), "Thermal buckling and post-buckling response of imperfect temperature-dependent sandwich FGM plates resting on elastic foundation", *Arch. Appl. Mech.*, **82**, 891-905.

Kraus, J. (1984), *Electromagnetics*, McGrawHill, Inc., USA.

Lei, Z.X., Zhang, L.W. and Liew, K.M. (2015a), "Free vibration analysis of laminated FG-CNT reinforced composite rectangular plates using the kp-Ritz method", *Compos. Struct.*, **127**, 245-259.

Lei, Z.X., Zhang, L.W. and Liew, K.M. (2015b), "Elastodynamic analysis of carbon nanotube-reinforced functionally graded plates", *Int. J. Mech. Sci.*, **99**, 206-217, 2015.

Lei, Z.X., Zhang, L.W. and Liew, K.M. (2016), "Analysis of laminated CNT reinforced functionally graded plates using the element-free kp-Ritz method", *Compos. Part B*, **84**, 211-221.

Lei, Z.X., Zhang, L.W., Liew, K.M. and Yu, J.L. (2014), "Dynamic stability analysis of carbon nanotube-reinforced functionally graded cylindrical panels using the element-free kp-Ritz method", *Compos. Struct.*, **113**, 328-338.

Liew, K.M., Zhang, Y. and Zhang, L.W. (2017), "Nonlocal elasticity theory for graphene modeling and simulation: prospects and challenges", *J. Model. Mech. Mater.*, DOI: https://doi.org/10.1515/jmmm-2016-0159.

Liu, M., Cheng, Y. and Liu, J. (2015), "High-order free vibration analysis of sandwich plates with both functionally graded face sheets and functionally graded flexible core", *Compos. Part B*, **72**, 97-107.

Mantari, J.L., Oktem, A.S. and Guedes Soares, C. (2012), "A new trigonometric shear deformation theory for isotropic, laminated composite and sandwich plates", *Int. J. Solid. Struct.*, **49**, 43-53.

Marynowski, K. (2012), "Dynamic analysis of an axially moving sandwich beam with viscoelastic core", *Compos. Struct.*, **94**, 2931-2936.

Mohammadimehr, M., Mohandes, M. and Moradi, M. (2016a), "Size dependent effect on the buckling and vibration analysis of double-bonded nanocomposite piezoelectric plate reinforced by boron nitride nanotube based on modified couple stress theory", *J. Vib. Control*, **22**(7), 1790-1807.

Mohammadimehr, M. and Mostafavifar, M. (2016), "Free vibration analysis of sandwich plate with a transversely flexible core and FG-CNTs reinforced nanocomposite face sheets subjected to magnetic field and temperature-dependent material properties using SGT", *Compos. Part B*, **94**, 253-270.

Mohammadimehr, M., Rostami, R. and Arefi, M. (2016b), "Electro-elastic analysis of a sandwich thick plate considering FG core and composite piezoelectric layers on Pasternak foundation using TSDT", *Steel Compos. Struct.*, **20**(3), 513-543.

Mohammadimehr, M., Rousta Navi, B. and Ghorbanpour Arani, A. (2015), "Free vibration of viscoelastic double-bonded polymeric nanocomposite plates reinforced by FG-SWCNTs using MSGT, sinusoidal shear deformation theory and meshless method", *Compos. Struct.*, **131**, 654-671.

Mohammadimehr, M., Rousta Navi, B. and Ghorbanpour Arani, A. (2016c), "Modified strain gradient Reddy rectangular plate model for biaxial buckling and bending analysis of double-coupled piezoelectric polymeric nanocomposite reinforced by FG-SWNT", *Compos. Part B*, **87**, 132-148.

Mohammadimehr, M., Salemi, M. and Rousta Navi, B. (2016d), "Bending, buckling, and free vibration analysis of MSGT microcomposite Reddy plate reinforced by FG-SWCNTs with temperature- dependent material properties under hydro-thermo-mechanical loadings using DQM", *Compos. Struct.*, **138**, 361-380.

Natarajan, S., Haboussi, M. and Manickam, G. (2014), "Application of higher-order structural theory to bending and free vibration analysis of sandwich plates with CNT reinforced composite facesheets", *Compos. Struct.*, **113**, 197-207.

Nayak, A.K., Moy, S.S.J. and Shenoi, R.A. (2002), "Free vibration analysis of composite sandwich plates based on Reddy's higher-order theory", *Compos. Part B*, **33**, 505-519.

Pietrzakowski, M. (2008), "Piezoelectric control of composite plate vibration: Effect of electric potential distribution", *Comput. Struct.*, **86**, 948-954.

Sahoo, R. and Singh, B.N. (2014), "A new trigonometric zigzag theory for static analysis of laminated composite and sandwich plates", *Aerosp. Sci. Technol.*, **35**, 15-28.

Sayyad, A.S. and Ghugal, Y.M. (2015), "On the free vibration analysis of laminated composite and sandwich plates: A review of recent literature with some numerical results", *Compos. Struct.*, **129**, 177-201.

Tounsi, A., Houari, M.S.A. and Bessaim, A. (2017), "A new 3-unknowns non-polynomial plate theory for buckling and vibration of functionally graded sandwich plate", *Struct. Eng. Mech.*, **60**(4), 547-565.

Viet, N.V., Wang, Q. and Kuo, W.S. (2017), "A studying on load transfer in carbon nanotube/epoxy composites under tension", *J. Model. Mech. Mater.*, DOI: https://doi.org/10.1515/jmmm-2016-0153.

Wang, Z.X and Shen, H.S. (2012), "Nonlinear vibration and bending of sandwich plates with nanotube-reinforced composite face sheets", *Compos. Part B*, **43**, 411-421.

Wang, T., Sokolinsky, V., Rajaram, S. and Nutt, S.R. (2008), "Consistent higher-order free vibration analysis of composite sandwich plates", *Compos. Struct.*, **82**, 609-621.

Zenkour, A.M. (2005), "A comprehensive analysis of functionally graded sandwich plates: Part 2-Buckling and free vibration", *Int. J. Solid. Struct.*, **42**, 5243-5258.

Zenkour, A.M. and Alghamdi, N.A. (2010), "Bending analysis of functionally graded sandwich plates under the effect of mechanical and thermal loads", *Mech. Adv. Mater. Struct.*, **17**, 419-432.

Zhang, L.W. (2017a), "An element-free based IMLS-Ritz method for buckling analysis of nanocomposite plates of polygonal planform", *Eng. Anal. Bound. Elem.*, **77**, 10-25.

Zhang, L.W. (2017c), "On the study of the effect of in-plane forces on the frequency parameters of CNT-reinforced composite skew plates", *Compos. Struct.*, **160**, 824-837.

Zhang, L.W., Cui, W.C. and Liew, K.M. (2015a), "Vibration

analysis of functionally graded carbon nanotube reinforced composite thick plates with elastically restrained edges", *Int. J. Mech. Sci.*, **103**, 9-21.
Zhang, L.W., Lei, Z.X. and Liew, K.M. (2015b), "Buckling analysis of FG-CNT reinforced composite thick skew plates using an element-free approach", *Compos. Part B*, **75**, 36-46.
Zhang, L.W., Li, D.M. and Liew, K.M. (2015c), "An element-free computational framework for elastodynamic problems based on the IMLS-Ritz method", *Eng. Anal. Bound. Elem.*, **54**, 39-46.
Zhang, L.W. and Liew, K.M. (2015a), "Geometrically nonlinear large deformation analysis of functionally graded carbon nanotube reinforced composite straight-sided quadrilateral plates", *Comput. Meth. Appl. Mech. Eng.*, **295**, 219-239.
Zhang, L.W. and Liew, K.M. (2015b), "Large deflection analysis of FG-CNT reinforced composite skew plates resting on Pasternak foundations using an element-free approach", *Compos. Struct.*, **132**, 974-993.
Zhang, L.W. and Liew, K.M. (2016a), "Postbuckling analysis of axially compressed CNT reinforced functionally graded composite plates resting on Pasternak foundations using an element-free approach", *Compos. Struct.*, **138**, 40-51.
Zhang, L.W. and Liew, K.M. (2016b), "Element-free geometrically nonlinear analysis of quadrilateral functionally graded material plates with internal column supports", *Compos. Struct.*, **147**, 99-110.
Zhang, L.W., Liew, K.M. and Jiang, Z. (2016a), "An element-free analysis of CNT-reinforced composite plates with column supports and elastically restrained edges under large deformation", *Compos. Part B*, **95**, 18-28.
Zhang, L.W., Liew, K.M. and Reddy, J.N. (2016b), "Postbuckling analysis of bi-axially compressed laminated nanocomposite plates using the first-order shear deformation theory", *Compos. Struct.*, **152**, 418-431.
Zhang, L.W., Liew, K.M. and Reddy, J.N. (2016c), "Postbuckling behavior of bi-axially compressed arbitrarily straight-sided quadrilateral functionally graded material plates", *Comput. Meth. Appl. Mech. Eng.*, **300**, 593-610.
Zhang, L.W., Liew, K.M. and Reddy, J.N. (2016d), "Postbuckling of carbon nanotube reinforced functionally graded plates with edges elastically restrained against translation and rotation under axial compression", *Comput. Meth. Appl. Mech. Eng.*, **298**, 1-28.
Zhang, L.W., Liu, W.H. and Liew, K.M. (2016e), "Geometrically nonlinear large deformation analysis of triangular CNT-reinforced composite plates", *Int. J. Nonlin. Mech.*, **86**, 122-132.
Zhang, L.W., Song, Z.G. and Liew, K.M. (2015d), "Nonlinear bending analysis of FG-CNT reinforced composite thick plates resting on Pasternak foundations using the element-free IMLS-Ritz method", *Compos. Struct.*, **128**, 165-175.
Zhang, L.W., Song, Z.G. and Liew, K.M. (2015e), "State-space Levy method for vibration analysis of FG-CNT composite plates subjected to in-plane loads based on higher-order shear deformation theory", *Compos. Struct.*, **134**, 989-1003.
Zhang, L.W., Song, Z.G. and Liew, K.M. (2015f), "State-space Levy method for vibration analysis of FG-CNT composite plates subjected to in-plane loads based on higher-order shear deformation theory", *Compos. Struct.*, **134**, 989-1003.
Zhang, L.W., Song, Z.G. and Liew, K.M. (2016f), "Computation of aerothermoelastic properties and active flutter control of CNT reinforced functionally graded composite panels in supersonic airflow", *Comput. Meth. Appl. Mech. Eng.*, **300**, 427-441.
Zhang, L.W., Song, Z.G. and Liew, K.M. (2016g), "Optimal shape control of CNT reinforced functionally graded composite plates using piezoelectric patches", *Compos. Part B*, **85**, 140-149.
Zhang, L.W., Song, Z.G., Qiao, P. and Liew, K.M. Liew, K.M. (2017), "Modeling of dynamic responses of CNT-reinforced composite cylindrical shells under impact loads", *Comput. Meth. Appl. Mech. Eng.*, **313**, 889-903.
Zhang, L.W., Xiao, L.N., Zou, G.L. and Liew, K.M. (2016h), "Elastodynamic analysis of quadrilateral CNT-reinforced functionally graded composite plates using FSDT element-free method", *Compos. Struct.*, **148**, 144-154.
Zhang, L.W., Zhang, Y., Zou, G.L. and Liew, K.M. (2016i), "Free vibration analysis of triangular CNT-reinforced composite plates subjected to in-plane stresses using FSDT element-free method", *Compos. Struct.*, **149**, 247-260.
Zhang, L.W., Zhu, P. and Liew, K.M. (2014), "Thermal buckling of functionally graded plates using a local Kriging meshless method", *Compos. Struct.*, **108**, 472-492.
Zhang. L.W. (2017b), "Geometrically nonlinear large deformation of CNT-reinforced composite plates with internal column supports", *J. Model. Mech. Mater.*, DOI: https://doi.org/10.1515/jmmm-2016-0154.
Zhu, P., Zhang, L.W. and Liew, K.M. (2014), "Geometrically nonlinear thermomechanical analysis of moderately thick functionally graded plates using a local Petrov-Galerkin approach with moving Kriging interpolation", *Compos. Struct.*, **107**, 298-314.
Zhu, P., Lei, Z.X. and Liew, K.M. (2012), "Static and free vibration analyses of carbon nanotube-reinforced composite plates using finite element method with first order shear deformation plate theory", *Compos. Struct.*, **94**, 1450-1460.

CC

Appendix A

$$\gamma_x = -z\left(\frac{\partial^3 w}{\partial x^3}+\frac{\partial^3 w}{\partial y^2\partial x}\right)+\psi(z)\left(\frac{\partial^2\phi_x}{\partial x^2}+\frac{\partial^2\phi_y}{\partial y\,\partial x}\right), \tag{A-1}$$

$$\gamma_y = -z\left(\frac{\partial^3 w}{\partial y\,\partial x^2}+\frac{\partial^3 w}{\partial y^3}\right)+\psi(z)\left(\frac{\partial^2\phi_x}{\partial y\,\partial x}+\frac{\partial^2\phi_y}{\partial y^2}\right), \tag{A-2}$$

$$\gamma_z = -\frac{\partial^2 w}{\partial x^2}-\frac{\partial^2 w}{\partial y^2}+\left(\frac{d}{dz}\psi(z)\right)\left(\frac{\partial\phi_x}{\partial x}+\frac{\partial\phi_y}{\partial y}\right), \tag{A-3}$$

$$\eta^{(1)}_{xxx} = \frac{z}{5}\left(-2\frac{\partial^3 w}{\partial x^3}+3\frac{\partial^3 w}{\partial y^2\partial x}\right)+\frac{\psi(z)}{5}\left(2\frac{\partial^2\phi_x}{\partial x^2}-2\frac{\partial^2\phi_y}{\partial y\,\partial x}-\frac{\partial^2\phi_x}{\partial y^2}\right) -\frac{1}{5}\left(\frac{d^2}{dz^2}\psi(z)\right)\phi_x, \tag{A-4}$$

$$\eta^{(1)}_{xxy} = \eta^{(1)}_{xyx} = \eta^{(1)}_{yxx} = \frac{z}{5}\left(-4\frac{\partial^3 w}{\partial y\,\partial x^2}+\frac{\partial^3 w}{\partial y^3}\right) +\frac{\psi(z)}{15}\left(4\frac{\partial^2\phi_y}{\partial x^2}+8\frac{\partial^2\phi_x}{\partial y\,\partial x}-3\frac{\partial^2\phi_y}{\partial y^2}\right)-\frac{1}{15}\left(\frac{d^2}{dz^2}\psi(z)\right)\phi_y, \tag{A-5}$$

$$\eta^{(1)}_{xxz} = \eta^{(1)}_{xzx} = \eta^{(1)}_{zxx} = -\frac{4}{15}\frac{\partial^2 w}{\partial x^2}+\frac{1}{15}\frac{\partial^2 w}{\partial y^2} +\frac{2}{15}\left(\frac{d}{dz}\psi(z)\right)\left(4\frac{\partial\phi_x}{\partial x}-\frac{\partial\phi_y}{\partial y}\right), \tag{A-6}$$

$$\eta^{(1)}_{xyy} = \eta^{(1)}_{yxy} = \eta^{(1)}_{yyx} = \frac{z}{5}\left(\frac{\partial^3 w}{\partial x^3}-4\frac{\partial^3 w}{\partial y^2\partial x}\right) +\frac{\psi(z)}{15}\left(8\frac{\partial^2\phi_y}{\partial y\,\partial x}+4\frac{\partial^2\phi_x}{\partial y^2}-3\frac{\partial^2\phi_x}{\partial x^2}\right)-\frac{1}{15}\left(\frac{d^2}{dz^2}\psi(z)\right)\phi_x, \tag{A-7}$$

$$\eta^{(1)}_{yyy} = \frac{z}{5}\left(3\frac{\partial^3 w}{\partial y\,\partial x^2}-2\frac{\partial^3 w}{\partial y^3}\right)+\frac{\psi(z)}{5}\left(2\frac{\partial^2\phi_y}{\partial y^2}-2\frac{\partial^2\phi_x}{\partial y\,\partial x}-\frac{\partial^2\phi_y}{\partial x^2}\right) -\frac{1}{5}\left(\frac{d^2}{dz^2}\psi(z)\right)\phi_y, \tag{A-8}$$

$$\eta^{(1)}_{yyz} = \eta^{(1)}_{yzy} = \eta^{(1)}_{zyy} = -\frac{4}{15}\frac{\partial^2 w}{\partial y^2}+\frac{1}{15}\frac{\partial^2 w}{\partial x^2} +\frac{2}{15}\left(\frac{d}{dz}\psi(z)\right)\left(4\frac{\partial\phi_y}{\partial y}-\frac{\partial\phi_x}{\partial x}\right), \tag{A-9}$$

$$\eta^{(1)}_{yzz} = \eta^{(1)}_{zyz} = \eta^{(1)}_{zzy} = \frac{z}{5}\left(\frac{\partial^3 w}{\partial y\,\partial x^2}+\frac{\partial^3 w}{\partial y^3}\right) -\frac{\psi(z)}{15}\left(2\frac{\partial^2\phi_x}{\partial y\,\partial x}+3\frac{\partial^2\phi_y}{\partial y^2}+\frac{\partial^2\phi_y}{\partial x^2}\right)+\frac{4}{15}\left(\frac{d^2}{dz^2}\psi(z)\right)\phi_y, \tag{A-10}$$

$$\eta^{(1)}_{xzz} = \eta^{(1)}_{zxz} = \eta^{(1)}_{zzx} = \frac{z}{5}\left(\frac{\partial^3 w}{\partial x^3}+\frac{\partial^3 w}{\partial y^2\partial x}\right) -\frac{\psi(z)}{15}\left(3\frac{\partial^2\phi_x}{\partial x^2}+2\frac{\partial^2\phi_y}{\partial y\,\partial x}+\frac{\partial^2\phi_x}{\partial y^2}\right)+\frac{4}{15}\left(\frac{d^2}{dz^2}\psi(z)\right)\phi_x, \tag{A-11}$$

$$\eta^{(1)}_{xyz} = \eta^{(1)}_{yzx} = \eta^{(1)}_{zxy} = \eta^{(1)}_{xzy} = \eta^{(1)}_{zyx} = \eta^{(1)}_{yxz} = -\frac{1}{3}\frac{\partial^2 w}{\partial y\,\partial x} +\frac{1}{3}\left(\frac{d}{dz}\psi(z)\right)\left(\frac{\partial\phi_y}{\partial x}+\frac{\partial\phi_x}{\partial y}\right), \tag{A-12}$$

$$\eta^{(1)}_{zzz} = \frac{1}{5}\frac{\partial^2 w}{\partial x^2}+\frac{1}{5}\frac{\partial^2 w}{\partial y^2}-\frac{2}{5}\left(\frac{d}{dz}\psi(z)\right)\left(\frac{\partial\phi_x}{\partial x}+\frac{\partial\phi_y}{\partial y}\right), \tag{A-13}$$

$$\chi_{xx} = \frac{\partial^2 w}{\partial y\,\partial x}-\frac{1}{2}\left(\frac{d}{dz}\psi(z)\right)\frac{\partial\phi_y}{\partial x}, \tag{A-14}$$

$$\chi_{yy} = -\frac{\partial^2 w}{\partial y\,\partial x}+\frac{1}{2}\left(\frac{d}{dz}\psi(z)\right)\frac{\partial\phi_x}{\partial y}, \tag{A-15}$$

$$\chi_{zz} = \frac{1}{2}\left(\frac{d}{dz}\psi(z)\right)\left(\frac{\partial\phi_y}{\partial x}-\frac{\partial\phi_x}{\partial y}\right), \tag{A-16}$$

$$\chi_{xy} = \chi_{yx} = \frac{1}{2}\frac{\partial^2 w}{\partial y^2}-\frac{1}{2}\frac{\partial^2 w}{\partial x^2}+\frac{1}{4}\left(\frac{d}{dz}\psi(z)\right)\left(\frac{\partial\phi_x}{\partial x}-\frac{\partial\phi_y}{\partial y}\right), \tag{A-17}$$

$$\chi_{xz} = \chi_{zx} = \frac{1}{4}\psi(z)\left(\frac{\partial^2\phi_y}{\partial x^2}-\frac{\partial^2\phi_x}{\partial y\,\partial x}\right)-\frac{1}{4}\left(\frac{d^2}{dz^2}\psi(z)\right)\phi_y, \tag{A-18}$$

$$\chi_{yz} = \chi_{zy} = \frac{1}{4}\psi(z)\left(\frac{\partial^2\phi_y}{\partial y\,\partial x}-\frac{\partial^2\phi_x}{\partial y^2}\right)+\frac{1}{4}\left(\frac{d^2}{dz^2}\psi(z)\right)\phi_x, \tag{A-19}$$

Appendix B

$$A^s_{pq} = A^{c-s}_{pq}+A^{f-s}_{pq} = \int_{-h/2}^{h/2}\left(Q^s_{pq}z^2\right)dz = \int_{-\frac{h_c}{2}}^{\frac{h_c}{2}}\left(Q^{c-s}_{pq}z^2\right)dz +\left[\int_{-\frac{h_c}{2}-h_f}^{-\frac{h_c}{2}}\left(Q^{f-s}_{pq}z^2\right)dz+\int_{\frac{h_c}{2}}^{\frac{h_c}{2}+h_f}\left(Q^{f-s}_{pq}z^2\right)dz\right], \tag{B-1}$$

$$B^s_{pq} = B^{c-s}_{pq}+B^{f-s}_{pq} = \int_{-h/2}^{h/2}\left(Q^s_{pq}\psi(z)^2\right)dz = \int_{-\frac{h_c}{2}}^{\frac{h_c}{2}}\left(Q^{c-s}_{pq}\psi(z)^2\right)dz +\left[\int_{-\frac{h_c}{2}-h_f}^{-\frac{h_c}{2}}\left(Q^{f-s}_{pq}\psi(z)^2\right)dz+\int_{\frac{h_c}{2}}^{\frac{h_c}{2}+h_f}\left(Q^{f-s}_{pq}\psi(z)^2\right)dz\right], \tag{B-2}$$

$$D^s_{pq} = D^{c-s}_{pq}+D^{f-s}_{pq} = \int_{-h/2}^{h/2}\left(Q^s_{pq}z\,\psi(z)\right)dz = \int_{-\frac{h_c}{2}}^{\frac{h_c}{2}}\left(Q^{c-s}_{pq}z\,\psi(z)\right)dz +\left[\int_{-\frac{h_c}{2}-h_f}^{-\frac{h_c}{2}}\left(Q^{f-s}_{pq}z\,\psi(z)\right)dz+\int_{\frac{h_c}{2}}^{\frac{h_c}{2}+h_f}\left(Q^{f-s}_{pq}z\,\psi(z)\right)dz\right], \tag{B-3}$$

$$C^s_{bd} = C^{c-s}_{bd}+C^{f-s}_{bd} = \int_{-h/2}^{h/2}\left(Q^s_{bd}\left(\frac{d\psi(z)}{dz}\right)^2\right)dz = \int_{-\frac{h_c}{2}}^{\frac{h_c}{2}}\left(Q^{c-s}_{bd}\left(\frac{d\psi(z)}{dz}\right)^2\right)dz +\left[\int_{-\frac{h_c}{2}-h_f}^{-\frac{h_c}{2}}\left(Q^{f-s}_{bd}\left(\frac{d\psi(z)}{dz}\right)^2\right)dz+\int_{\frac{h_c}{2}}^{\frac{h_c}{2}+h_f}\left(Q^{f-s}_{bd}\left(\frac{d\psi(z)}{dz}\right)^2\right)dz\right], \tag{B-4}$$

$$I^s_0 = I^{c-s}_0+I^{f-s}_0 = \int_{-h/2}^{h/2}\left(\rho^s\right)dz = \int_{-\frac{h_c}{2}}^{\frac{h_c}{2}}\left(\rho^{c-s}\right)dz +\left[\int_{-\frac{h_c}{2}-h_f}^{-\frac{h_c}{2}}\left(\rho^{f-s}\right)dz+\int_{\frac{h_c}{2}}^{\frac{h_c}{2}+h_f}\left(\rho^{f-s}\right)dz\right], \tag{B-5}$$

$$I^s_2 = I^{c-s}_2+I^{f-s}_2 = \int_{-h/2}^{h/2}\left(\rho^s z^2\right)dz = \int_{-\frac{h_c}{2}}^{\frac{h_c}{2}}\left(\rho^{c-s}z^2\right)dz +\left[\int_{-\frac{h_c}{2}-h_f}^{-\frac{h_c}{2}}\left(\rho^{f-s}z^2\right)dz+\int_{\frac{h_c}{2}}^{\frac{h_c}{2}+h_f}\left(\rho^{f-s}z^2\right)dz\right], \tag{B-6}$$

$$I_3^s = I_3^{c-s} + I_3^{f-s} = \int_{-h/2}^{h/2} \left(\rho^s z\psi(z)\right)dz = \int_{-\frac{h_c}{2}}^{\frac{h_c}{2}} \left(\rho^{c-s} z\psi(z)\right)dz + \left[\int_{-\frac{h_c}{2}-h_f}^{-\frac{h_c}{2}} \left(\rho^{f-s} z\psi(z)\right)dz + \int_{\frac{h_c}{2}}^{\frac{h_c}{2}+h_f} \left(\rho^{f-s} z\psi(z)\right)dz\right], \tag{B-7}$$

$$I_4^s = I_4^{c-s} + I_4^{f-s} = \int_{-h/2}^{h/2} \left(\rho^s \psi(z)^2\right)dz = \int_{-\frac{h_c}{2}}^{\frac{h_c}{2}} \left(\rho^{c-s} \psi(z)^2\right)dz + \left[\int_{-\frac{h_c}{2}-h_f}^{-\frac{h_c}{2}} \left(\rho^{f-s} \psi(z)^2\right)dz + \int_{\frac{h_c}{2}}^{\frac{h_c}{2}+h_f} \left(\rho^{f-s} \psi(z)^2\right)dz\right], \tag{B-8}$$

$$G_0^s = G_0^{c-s} + G_0^{f-s} = \int_{-h/2}^{h/2} \left(G^s\right)dz = \int_{-\frac{h_c}{2}}^{\frac{h_c}{2}} \left(G^{c-s}\right)dz + \left[\int_{-\frac{h_c}{2}-h_f}^{-\frac{h_c}{2}} \left(G^{f-s}\right)dz + \int_{\frac{h_c}{2}}^{\frac{h_c}{2}+h_f} \left(G^{f-s}\right)dz\right], \tag{B-9}$$

$$G_1^s = G_1^{c-s} + G_1^{f-s} = \int_{-h/2}^{h/2} \left(G^s z\right)dz = \int_{-\frac{h_c}{2}}^{\frac{h_c}{2}} \left(G^{c-s} z\right)dz + \left[\int_{-\frac{h_c}{2}-h_f}^{-\frac{h_c}{2}} \left(G^{f-s} z\right)dz + \int_{\frac{h_c}{2}}^{\frac{h_c}{2}+h_f} \left(G^{f-s} z\right)dz\right], \tag{B-10}$$

$$G_2^s = G_2^{c-s} + G_2^{f-s} = \int_{-h/2}^{h/2} \left(G^s z^2\right)dz = \int_{-\frac{h_c}{2}}^{\frac{h_c}{2}} \left(G^{c-s} z^2\right)dz + \left[\int_{-\frac{h_c}{2}-h_f}^{-\frac{h_c}{2}} \left(G^{f-s} z^2\right)dz + \int_{\frac{h_c}{2}}^{\frac{h_c}{2}+h_f} \left(G^{f-s} z^2\right)dz\right], \tag{B-11}$$

$$G_3^s = G_3^{c-s} + G_3^{f-s} = \int_{-h/2}^{h/2} \left(G^s z\psi(z)\right)dz = \int_{-\frac{h_c}{2}}^{\frac{h_c}{2}} \left(G^{c-s} z\psi(z)\right)dz + \left[\int_{-\frac{h_c}{2}-h_f}^{-\frac{h_c}{2}} \left(G^{f-s} z\psi(z)\right)dz + \int_{\frac{h_c}{2}}^{\frac{h_c}{2}+h_f} \left(G^{f-s} z\psi(z)\right)dz\right], \tag{B-12}$$

$$G_4^s = G_4^{c-s} + G_4^{f-s} = \int_{-h/2}^{h/2} \left(G^s \psi(z)^2\right)dz = \int_{-\frac{h_c}{2}}^{\frac{h_c}{2}} \left(G^{c-s} \psi(z)^2\right)dz + \left[\int_{-\frac{h_c}{2}-h_f}^{-\frac{h_c}{2}} \left(G^{f-s} \psi(z)^2\right)dz + \int_{\frac{h_c}{2}}^{\frac{h_c}{2}+h_f} \left(G^{f-s} \psi(z)^2\right)dz\right], \tag{B-13}$$

$$G_5^s = G_5^{c-s} + G_5^{f-s} = \int_{-h/2}^{h/2} \left(G^s \left(\frac{d\psi(z)}{dz}\right)\right)dz = \int_{-\frac{h_c}{2}}^{\frac{h_c}{2}} \left(G^{c-s} \left(\frac{d\psi(z)}{dz}\right)\right)dz + \left[\int_{-\frac{h_c}{2}-h_f}^{-\frac{h_c}{2}} \left(G^{f-s} \left(\frac{d\psi(z)}{dz}\right)\right)dz + \int_{\frac{h_c}{2}}^{\frac{h_c}{2}+h_f} \left(G^{f-s} \left(\frac{d\psi(z)}{dz}\right)\right)dz\right], \tag{B-14}$$

$$G_6^s = G_6^{c-s} + G_6^{f-s} = \int_{-h/2}^{h/2} \left(G^s \left(\frac{d\psi(z)}{dz}\right)^2\right)dz = \int_{-\frac{h_c}{2}}^{\frac{h_c}{2}} \left(G^{c-s} \left(\frac{d\psi(z)}{dz}\right)^2\right)dz + \left[\int_{-\frac{h_c}{2}-h_f}^{-\frac{h_c}{2}} \left(G^{f-s} \left(\frac{d\psi(z)}{dz}\right)^2\right)dz + \int_{\frac{h_c}{2}}^{\frac{h_c}{2}+h_f} \left(G^{f-s} \left(\frac{d\psi(z)}{dz}\right)^2\right)dz\right], \tag{B-15}$$

$$G_7^s = G_7^{c-s} + G_7^{f-s} = \int_{-h/2}^{h/2} \left(G^s \left(\frac{d^2\psi(z)}{dz^2}\right)\right)dz = \int_{-\frac{h_c}{2}}^{\frac{h_c}{2}} \left(G^{c-s} \left(\frac{d^2\psi(z)}{dz^2}\right)\right)dz + \left[\int_{-\frac{h_c}{2}-h_f}^{-\frac{h_c}{2}} \left(G^{f-s} \left(\frac{d^2\psi(z)}{dz^2}\right)\right)dz + \int_{\frac{h_c}{2}}^{\frac{h_c}{2}+h_f} \left(G^{f-s} \left(\frac{d^2\psi(z)}{dz^2}\right)\right)dz\right], \tag{B-16}$$

$$G_8^s = G_8^{c-s} + G_8^{f-s} = \int_{-h/2}^{h/2} \left(G^s \left(\frac{d^2\psi(z)}{dz^2}\right)^2\right)dz = \int_{-\frac{h_c}{2}}^{\frac{h_c}{2}} \left(G^{c-s} \left(\frac{d^2\psi(z)}{dz^2}\right)^2\right)dz + \left[\int_{-\frac{h_c}{2}-h_f}^{-\frac{h_c}{2}} \left(G^{f-s} \left(\frac{d^2\psi(z)}{dz^2}\right)^2\right)dz + \int_{\frac{h_c}{2}}^{\frac{h_c}{2}+h_f} \left(G^{f-s} \left(\frac{d^2\psi(z)}{dz^2}\right)^2\right)dz\right], \tag{B-17}$$

$$G_9^s = G_9^{c-s} + G_9^{f-s} = \int_{-h/2}^{h/2} \left(G^s z \left(\frac{d^2\psi(z)}{dz^2}\right)\right)dz = \int_{-\frac{h_c}{2}}^{\frac{h_c}{2}} \left(G^{c-s} z \left(\frac{d^2\psi(z)}{dz^2}\right)\right)dz + \left[\int_{-\frac{h_c}{2}-h_f}^{-\frac{h_c}{2}} \left(G^{f-s} z \left(\frac{d^2\psi(z)}{dz^2}\right)\right)dz + \int_{\frac{h_c}{2}}^{\frac{h_c}{2}+h_f} \left(G^{f-s} z \left(\frac{d^2\psi(z)}{dz^2}\right)\right)dz\right], \tag{B-18}$$

$$S_1 = \int_{-\frac{h_c}{2}-h_f}^{-\frac{h_c}{2}} dz + \int_{\frac{h_c}{2}}^{\frac{h_c}{2}+h_f} dz, \tag{B-19}$$

$$S_2 = \int_{-\frac{h_c}{2}-h_f}^{-\frac{h_c}{2}} \left(z^2\right)dz + \int_{\frac{h_c}{2}}^{\frac{h_c}{2}+h_f} \left(z^2\right)dz, \tag{B-20}$$

$$S_3 = \int_{-\frac{h_c}{2}-h_f}^{-\frac{h_c}{2}} \left(z\psi(z)\right)dz + \int_{\frac{h_c}{2}}^{\frac{h_c}{2}+h_f} \left(z\psi(z)\right)dz, \tag{B-21}$$

$$S_4 = \int_{-\frac{h_c}{2}-h_f}^{-\frac{h_c}{2}} \left(\psi(z)^2\right)dz + \int_{\frac{h_c}{2}}^{\frac{h_c}{2}+h_f} \left(\psi(z)^2\right)dz, \tag{B-22}$$

$$S_5 = \int_{-\frac{h_c}{2}-h_f}^{-\frac{h_c}{2}} \left(\frac{d\psi(z)}{dz}\right)dz + \int_{\frac{h_c}{2}}^{\frac{h_c}{2}+h_f} \left(\frac{d\psi(z)}{dz}\right)dz, \tag{B-23}$$

$$P_1 = \int_{-\frac{h_c}{2}-h_f}^{-\frac{h_c}{2}} z\cos\left(\frac{\pi(-z-\frac{h_c}{2})}{h_f}\right)dz + \int_{\frac{h_c}{2}}^{\frac{h_c}{2}+h_f} z\cos\left(\frac{\pi(z-\frac{h_c}{2})}{h_f}\right)dz, \tag{B-24}$$

$$P_2 = \int_{-\frac{h_c}{2}-h_f}^{-\frac{h_c}{2}} \left(\frac{d\psi(z)}{dz}\right)\sin\left(\frac{\pi(-z-\frac{h_c}{2})}{h_f}\right)dz + \int_{\frac{h_c}{2}}^{\frac{h_c}{2}+h_f} \left(\frac{d\psi(z)}{dz}\right)\sin\left(\frac{\pi(z-\frac{h_c}{2})}{h_f}\right)dz, \tag{B-25}$$

$$P_3 = \int_{-\frac{h_c}{2}-h_f}^{-\frac{h_c}{2}} \cos\left(\frac{\pi(-z-\frac{h_c}{2})}{h_f}\right)^2 dz + \int_{\frac{h_c}{2}}^{\frac{h_c}{2}+h_f} \cos\left(\frac{\pi(z-\frac{h_c}{2})}{h_f}\right)^2 dz, \tag{B-26}$$

$$P_4 = \int_{-\frac{h_c}{2}-h_f}^{-\frac{h_c}{2}} \sin\left(\frac{\pi(-z-\frac{h_c}{2})}{h_f}\right)^2 dz + \int_{\frac{h_c}{2}}^{\frac{h_c}{2}+h_f} \sin\left(\frac{\pi(z-\frac{h_c}{2})}{h_f}\right)^2 dz, \tag{B-27}$$

$$P_5 = \int_{-\frac{h_c}{2}-h_f}^{-\frac{h_c}{2}} \psi(z)\cos\left(\frac{\pi(-z-\frac{h_c}{2})}{h_f}\right)dz + \int_{\frac{h_c}{2}}^{\frac{h_c}{2}+h_f} \psi(z)\cos\left(\frac{\pi(z-\frac{h_c}{2})}{h_f}\right)dz, \quad \text{(B-28)}$$

where *pq*=11,12,22,66 and *bd*=44,55.

Appendix C

The arrays of matrices *M*, *C* and *K* in Eq. (26) are defined as follows:

$$M_{11} = \overline{I_2^1}\pi^2\alpha\beta^2n^2 + \overline{I_2^1}\pi^2\alpha m^2 + \overline{I_0^1}\alpha, \quad \text{(C-1)}$$

$$C_{11} = C_d^*, \quad \text{(C-2)}$$

$$\begin{aligned}
K_{11} &= 4\overline{l_0^1}^2\overline{G_0^1}\alpha\beta^2m^2\pi^4n^2 + 2\overline{l_0^1}^2\overline{G_0^1}\alpha\beta^4n^4\pi^4 + 2\overline{l_0^1}^2\overline{G_2^1}\alpha\beta^6n^6\pi^6 \\
&+6\overline{l_0^1}^2\overline{G_2^1}\alpha\beta^2m^4\pi^6n^2 + 6\overline{l_0^1}^2\overline{G_2^1}\alpha\beta^4m^2\pi^6n^4 + 2\overline{l_0^1}^2\overline{G_0^1}\alpha m^4\pi^4 \\
&+2\overline{l_0^1}^2\overline{G_2^1}\alpha m^6\pi^6 + \frac{12}{5}\overline{l_1^1}^2\overline{G_2^1}\alpha\beta^4m^2\pi^6n^4 + \frac{16}{15}\overline{l_1^1}^2\overline{G_0^1}\alpha\beta^2m^2\pi^4n^2 \\
&+\frac{4}{5}\overline{l_1^1}^2\overline{G_2^1}\alpha\beta^6n^6\pi^6 + \frac{8}{15}\overline{l_1^1}^2\overline{G_0^1}\alpha\beta^4n^4\pi^4 + \frac{12}{5}\overline{l_1^1}^2\overline{G_2^1}\alpha\beta^2m^4\pi^6n^2 \\
&+\frac{8}{15}\overline{l_1^1}^2\overline{G_0^1}\alpha m^4\pi^4 + \frac{4}{5}\overline{l_1^1}^2\overline{G_2^1}\alpha m^6\pi^6 + 3\overline{l_2^1}^2\overline{G_0^1}\alpha\beta^2m^2\pi^4n^2 \\
&+\frac{1}{2}\overline{l_2^1}^2\overline{G_0^1}\alpha m^4\pi^4 + \frac{1}{2}\overline{l_2^1}^2\overline{G_0^1}\alpha\beta^4n^4\pi^4 + \overline{A_{11}^1}\alpha m^4\pi^4 + \overline{A_{22}^1}\alpha\beta^4n^4\pi^4 \\
&+4\overline{A_{66}^1}\alpha\beta^2m^2\pi^4n^2 + 2\overline{A_{12}^1}\alpha\beta^2m^2\pi^4n^2 + H^2H_x^{*2}\overline{S_2}\alpha m^4\pi^4 \\
&+H^2H_x^{*2}\overline{S_1}\alpha\beta^2n^2\pi^2 + H_x^{*2}\overline{S_2}\alpha\beta^2m^2\pi^4n^2 + H_x^{*2}\overline{S_2}\alpha\beta^4n^4\pi^4 \\
&-H^2H_x^{*2}\overline{S_1}\alpha m^2\pi^2 - H_x^{*2}\overline{S_1}\alpha\beta^2n^2\pi^2 + H_x^{*2}\overline{S_1}\alpha m^2\pi^2 \\
&+H^2H_x^{*2}\overline{S_2}\alpha\beta^2m^2\pi^4n^2 + \alpha k_1k_{w12}^* + \alpha k_{w12}^* + \alpha\beta^2k_Gk_{Gx}^*n^2\pi^2 \\
&+\alpha k_{Gx}^*m^2\pi^2,
\end{aligned} \quad \text{(C-3)}$$

$$M_{12} = -\overline{I_3^1}m\pi, \quad \text{(C-4)}$$

$$\begin{aligned}
K_{12} &= -2\overline{l_0^1}^2\overline{G_5^1}\beta^2m\pi^3n^2 - 2\overline{l_0^1}^2\overline{G_3^1}m^5\pi^5 - 2\overline{l_0^1}^2\overline{G_5^1}m^3\pi^3 \\
&-2\overline{l_0^1}^2\overline{G_3^1}\beta^4m\pi^5n^4 - 4\overline{l_0^1}^2\overline{G_3^1}\beta^2m^3\pi^5n^2 - \frac{16}{15}\overline{l_1^1}^2\overline{G_5^1}\beta^2m\pi^3n^2 \\
&-\frac{2}{5}\overline{l_1^1}^2\overline{G_9^1}m^3\pi^3 - \frac{4}{5}\overline{l_1^1}^2\overline{G_3^1}\beta^4m\pi^5n^4 - \frac{4}{5}\overline{l_1^1}^2\overline{G_3^1}m^5\pi^5 - \frac{16}{15}\overline{l_1^1}^2\overline{G_5^1}m^3\pi^3 \\
&-\frac{2}{5}\overline{l_1^1}^2\overline{G_7^1}\beta^2m\pi^3n^2 - \frac{8}{5}\overline{l_1^1}^2\overline{G_3^1}\beta^2m^3\pi^5n^2 - \frac{3}{4}\overline{l_2^1}^2\overline{G_5^1}\beta^2m\pi^3n^2 \\
&-\frac{1}{4}\overline{l_2^1}^2\overline{G_5^1}m^3\pi^3 - \overline{D_{11}^1}m^3\pi^3 - 2\overline{D_{12}^1}\beta^2m\pi^3n^2 - 2\overline{D_{66}^1}\beta^2m\pi^3n^2 \\
&-H^2H_x^{*2}\overline{S_3}\beta^2m\pi^3n^2 + \frac{1}{2}H^2H_x^{*2}\overline{S_5}m\pi - H^2H_x^{*2}\overline{S_3}m^3\pi^3,
\end{aligned} \quad \text{(C-5)}$$

$$M_{13} = -\overline{I_3^1}\beta n\pi, \quad \text{(C-6)}$$

$$\begin{aligned}
K_{13} &= -2\overline{l_0^1}^2\overline{G_3^1}\beta m^4\pi^5n - 4\overline{l_0^1}^2\overline{G_3^1}\beta^3m^2\pi^5n^3 - 2\overline{l_0^1}^2\overline{G_3^1}\beta^5n^5\pi^5 \\
&-2\overline{l_0^1}^2\overline{G_5^1}\beta^3n^3\pi^3 - 2\overline{l_0^1}^2\overline{G_5^1}\beta m^2\pi^3n - \frac{2}{5}\overline{l_1^1}^2\overline{G_9^1}\beta m^2\pi^3n \\
&-\frac{16}{15}\overline{l_1^1}^2\overline{G_5^1}\beta^3n^3\pi^3 - \frac{2}{5}\overline{l_1^1}^2\overline{G_7^1}\beta^3n^3\pi^3 - 4/5\overline{l_1^1}^2\overline{G_3^1}\beta^5n^5\pi^5 \\
&-\frac{4}{5}\overline{l_1^1}^2\overline{G_3^1}\beta m^4\pi^5n - \frac{16}{15}\overline{l_1^1}^2\overline{G_5^1}\beta m^2\pi^3n - \frac{8}{5}\overline{l_1^1}^2\overline{G_3^1}\beta^3m^2\pi^5n^3 \\
&-\frac{1}{4}\overline{l_2^1}^2\overline{G_5^1}\beta^3n^3\pi^3 - \frac{3}{4}\overline{l_2^1}^2\overline{G_5^1}\beta m^2\pi^3n - \overline{D_{22}^1}\beta^3n^3\pi^3 - \overline{D_{12}^1}\beta m^2\pi^3n \\
&-2\overline{D_{66}^1}\beta m^2\pi^3n - H_x^{*2}\overline{S_3}\beta m^2\pi^3n + \frac{1}{2}H_x^{*2}\overline{S_5}\beta n\pi - H_x^{*2}\overline{S_3}\beta^3n^3\pi^3,
\end{aligned} \quad \text{(C-7)}$$

$$C_{14} = -C_d^*, \quad \text{(C-8)}$$

$$K_{14} = -\alpha\beta^2k_Gk_{Gx}^*n^2\pi^2 - \alpha k_{Gx}^*m^2\pi^2 - \alpha k_{w12}^*, \quad \text{(C-9)}$$

$$M_{21} = -\overline{I_3^1}\alpha m\pi, \quad \text{(C-10)}$$

$$\begin{aligned}
K_{21} &= -2\overline{l_0^1}^2\overline{G_5^1}\alpha m^3\pi^3 - 2\overline{l_0^1}^2\overline{G_3^1}\alpha m^5\pi^5 - 2\overline{l_0^1}^2\overline{G_3^1}\beta^4\alpha m\pi^5n^4 \\
&-2\overline{l_0^1}^2\overline{G_5^1}\beta^2\alpha m\pi^3n^2 - 4\overline{l_0^1}^2\overline{G_3^1}\beta^2\alpha m^3\pi^5n^2 - \frac{4}{5}\overline{l_1^1}^2\overline{G_3^1}\alpha m^5\pi^5 \\
&-\frac{8}{5}\overline{l_1^1}^2\overline{G_3^1}\beta^2\alpha m^3\pi^5n^2 - \frac{16}{15}\overline{l_1^1}^2\overline{G_5^1}\beta^2\alpha m\pi^3n^2 - \frac{2}{5}\overline{l_1^1}^2\overline{G_7^1}\beta^2\alpha m\pi^3n^2 \\
&-\frac{4}{5}\overline{l_1^1}^2\overline{G_3^1}\beta^4\alpha m\pi^5n^4 - \frac{2}{5}\overline{l_1^1}^2\overline{G_9^1}\alpha m^3\pi^3 - \frac{16}{15}\overline{l_1^1}^2\overline{G_5^1}\alpha m^3\pi^3 \\
&-\frac{3}{4}\overline{l_2^1}^2\overline{G_5^1}\beta^2\alpha m\pi^3n^2 - \frac{1}{4}\overline{l_2^1}^2\overline{G_5^1}\alpha m^3\pi^3 - \overline{D_{11}^1}\alpha m^3\pi^3 \\
&-2\overline{D_{66}^1}\beta^2\alpha m\pi^3n^2 - 2\overline{D_{12}^1}\beta^2\alpha m\pi^3n^2 - H^2H_x^{*2}\overline{S_3}\beta^2\alpha m\pi^3n^2 \\
&+\frac{1}{2}H^2H_x^{*2}\overline{S_5}\alpha m\pi - H^2H_x^{*2}\overline{S_3}\alpha m^3\pi^3,
\end{aligned} \quad \text{(C-11)}$$

$$M_{22} = \overline{I_4^1}, \quad \text{(C-12)}$$

$$\begin{aligned}
K_{22} &= 2\overline{l_0^1}^2\overline{G_4^1}\beta^2m^2\pi^4n^2 + 2\overline{l_0^1}^2\overline{G_6^1}m^2\pi^2 + +2\overline{l_0^1}^2\overline{G_4^1}m^4\pi^4 \\
&+\frac{4}{5}\overline{l_1^1}^2\overline{G_7^1}m^2\pi^2 + \frac{4}{5}\overline{l_1^1}^2\overline{G_4^1}m^4\pi^4 + \frac{32}{15}\overline{l_1^1}^2\overline{G_6^1}m^2\pi^2 + \frac{4}{3}\overline{l_1^1}^2\overline{G_4^1}\beta^2m^2\pi^4n^2 \\
&+\frac{4}{15}\overline{l_1^1}^2\overline{G_7^1}\beta^2n^2\pi^2 + \frac{4}{3}\overline{l_1^1}^2\overline{G_6^1}\beta^2n^2\pi^2 + \frac{8}{15}\overline{l_1^1}^2\overline{G_4^1}\beta^4n^4\pi^4 + \frac{8}{15}\overline{l_1^1}^2\overline{G_8^1} \\
&+\frac{1}{8}\overline{l_2^1}^2\overline{G_8^1} + \frac{1}{8}\overline{l_2^1}^2\overline{G_4^1}\beta^2m^2\pi^4n^2 + \overline{l_2^1}^2\overline{G_6^1}\beta^2n^2\pi^2 + \frac{1}{8}\overline{l_2^1}^2\overline{G_4^1}\beta^4n^4\pi^4 \\
&+\frac{1}{4}\overline{l_2^1}^2\overline{G_7^1}\beta^2n^2\pi^2 + \frac{1}{8}\overline{l_2^1}^2\overline{G_6^1}m^2\pi^2 + \overline{C_{55}^1} + \overline{B_{11}^1}m^2\pi^2 \\
&+\overline{B_{66}^1}\beta^2n^2\pi^2 + H^2H_x^{*2}\overline{S_4}m^2\pi^2 + H^2H_x^{*2}\overline{S_4}\beta^2n^2\pi^2,
\end{aligned} \quad \text{(C-13)}$$

$$\begin{aligned}
K_{23} &= +2\overline{l_0^1}^2\overline{G_4^1}\beta^3m\pi^4n^3 + 2\overline{l_0^1}^2\overline{G_4^1}\beta m^3\pi^4n + 2\overline{l_0^1}^2\overline{G_6^1}\beta m\pi^2n \\
&+\frac{4}{15}\overline{l_1^1}^2\overline{G_4^1}\beta^3m\pi^4n^3 + \frac{4}{5}\overline{l_1^1}^2\overline{G_6^1}\beta m\pi^2n + \frac{4}{15}\overline{l_1^1}^2\overline{G_4^1}\beta m^3\pi^4n \\
&+\frac{8}{15}\overline{l_1^1}^2\overline{G_7^1}\beta m\pi^2n - \frac{1}{4}\overline{l_2^1}^2\overline{G_7^1}\beta m\pi^2n - \frac{1}{8}\overline{l_2^1}^2\overline{G_4^1}\beta m^3\pi^4n \\
&-\frac{1}{8}\overline{l_2^1}^2\overline{G_4^1}\beta^3m\pi^4n^3 - \frac{5}{8}\overline{l_2^1}^2\overline{G_6^1}\beta m\pi^2n + \overline{B_{66}^1}\beta m\pi^2n + \overline{B_{12}^1}\beta m\pi^2n,
\end{aligned} \quad \text{(C-14)}$$

$$M_{31} = -\overline{I_3^1}\alpha\beta n\pi, \quad \text{(C-15)}$$

$$\begin{aligned}
K_{31} &= -2\overline{l_0^1}^2\overline{G_5^1}\alpha\beta m^2\pi^3n - 2\overline{l_0^1}^2\overline{G_3^1}\alpha\beta^5n^5\pi^5 - 2\overline{l_0^1}^2\overline{G_5^1}\alpha\beta^3n^3\pi^3 \\
&-2\overline{l_0^1}^2\overline{G_3^1}\alpha\beta m^4\pi^5n - 4\overline{l_0^1}^2\overline{G_3^1}\alpha\beta^3m^2\pi^5n^3 - \frac{2}{5}\overline{l_1^1}^2\overline{G_7^1}\alpha\beta^3n^3\pi^3 \\
&-\frac{2}{5}\overline{l_1^1}^2\overline{G_9^1}\alpha\beta m^2\pi^3n - \frac{4}{5}\overline{l_1^1}^2\overline{G_3^1}\alpha\beta^5n^5\pi^5 - \frac{16}{15}\overline{l_1^1}^2\overline{G_5^1}\alpha\beta m^2\pi^3n \\
&-\frac{8}{5}\overline{l_1^1}^2\overline{G_3^1}\alpha\beta^3m^2\pi^5n^3 - \frac{16}{15}\overline{l_1^1}^2\overline{G_5^1}\alpha\beta^3n^3\pi^3 - \frac{4}{5}\overline{l_1^1}^2\overline{G_3^1}\alpha\beta m^4\pi^5n \\
&-\frac{3}{4}\overline{l_2^1}^2\overline{G_5^1}\alpha\beta m^2\pi^3n - \frac{1}{4}\overline{l_2^1}^2\overline{G_5^1}\alpha\beta^3n^3\pi^3 - \overline{D_{22}^1}\alpha\beta^3n^3\pi^3 - 2\overline{D_{66}^1}\alpha\beta m^2\pi^3n \\
&-\overline{D_{12}^1}\alpha\beta m^2\pi^3n + \frac{1}{2}H_x^{*2}\overline{S_5}\alpha\beta n\pi - H_x^{*2}\overline{S_3}\alpha\beta^3n^3\pi^3 - H_x^{*2}\overline{S_3}\alpha\beta m^2\pi^3n,
\end{aligned} \quad \text{(C-16)}$$

$$\begin{aligned}
K_{32} &= 2\overline{l_0^1}^2\overline{G_6^1}\beta m\pi^2n + 2\overline{l_0^1}^2\overline{G_4^1}\beta^3m\pi^4n^3 + 2\overline{l_0^1}^2\overline{G_4^1}\beta m^3\pi^4n \\
&+4/5\overline{l_1^1}^2\overline{G_6^1}\beta m\pi^2n + \frac{4}{15}\overline{l_1^1}^2\overline{G_4^1}\alpha\beta^3m\pi^4n^3 + \frac{8}{15}\overline{l_1^1}^2\overline{G_7^1}\beta m\pi^2n \\
&+\frac{4}{15}\overline{l_1^1}^2\overline{G_4^1}\beta m^3\pi^4n - \frac{1}{4}\overline{l_2^1}^2\overline{G_7^1}\beta m\pi^2n - \frac{5}{8}\overline{l_2^1}^2\overline{G_6^1}\beta m\pi^2n \\
&-\frac{1}{8}\overline{l_2^1}^2\overline{G_4^1}\beta^3m\pi^4n^3 - \frac{1}{8}\overline{l_2^1}^2\overline{G_4^1}\beta m^3\pi^4n + \overline{B_{66}^1}\beta m\pi^2n + \overline{B_{12}^1}\beta m\pi^2n,
\end{aligned} \quad \text{(C-17)}$$

$$M_{33} = \overline{I_4^1}, \quad \text{(C-18)}$$

$$K_{33}=2\overline{l_0^2}\,\overline{G_6^1}\beta^2n^2\pi^2+2\overline{l_0^2}\,\overline{G_4^1}\beta^4n^4\pi^4+2\overline{l_0^2}\,\overline{G_4^1}\beta^2m^2\pi^4n^2$$
$$+\frac{4}{5}\overline{l_1^2}\,\overline{G_7^1}\beta^2n^2\pi^2+\frac{4}{5}\overline{l_1^2}\,\overline{G_4^1}\beta^4n^4\pi^4+\frac{32}{15}\overline{l_1^2}\,\overline{G_6^1}\beta^2n^2\pi^2+\frac{8}{15}\overline{l_1^2}\,\overline{G_8^1}$$
$$+\frac{4}{15}\overline{l_1^2}\,\overline{G_7^1}m^2\pi^2+\frac{4}{3}\overline{l_1^2}\,\overline{G_4^1}\beta^2m^2\pi^4n^2+\frac{4}{3}\overline{l_1^2}\,\overline{G_6^1}m^2\pi^2+\frac{8}{15}\overline{l_1^2}\,\overline{G_4^1}m^4\pi^4$$
$$+\frac{1}{8}\overline{l_2^2}\,\overline{G_8^1}+\frac{1}{4}\overline{l_2^2}\,\overline{G_7^1}m^2\pi^2+\frac{1}{8}\overline{l_2^2}\,\overline{G_4^1}m^4\pi^4+\frac{1}{8}\overline{l_2^2}\,\overline{G_6^1}\beta^2n^2\pi^2$$
$$+\overline{l_2^2}\,\overline{G_6^1}m^2\pi^2+\frac{1}{8}\overline{l_2^2}\,\overline{G_4^1}\beta^2m^2\pi^4n^2+\overline{B_{22}^1}\beta^2n^2\pi^2+\overline{B_{66}^1}m^2\pi^2$$
$$+\overline{C_{44}^1}+H_x^{*2}\overline{S_4}m^2\pi^2+H_x^{*2}\overline{S_4}\beta^2n^2\pi^2, \tag{C-19}$$

$$C_{41}=-C_d^*, \tag{C-20}$$

$$K_{41}=-\alpha\beta^2k_Gk_{Gx}^*n^2\pi^2-\alpha k_{Gx}^*m^2\pi^2-\alpha k_{w12}^*, \tag{C-21}$$

$$M_{44}=\overline{I_2^2}\pi^2\alpha\beta^2n^2+\overline{I_2^2}\pi^2\alpha m^2+\overline{I_0^2}\alpha, \tag{C-22}$$

$$C_{44}=C_d^*, \tag{C-23}$$

$$K_{44}=4\overline{l_0^2}\,\overline{G_0^2}\alpha\beta^2m^2\pi^4n^2+2\overline{l_0^2}\,\overline{G_0^2}\alpha\beta^4n^4\pi^4+2\overline{l_0^2}\,\overline{G_2^2}\alpha\beta^6n^6\pi^6$$
$$+6\overline{l_0^2}\,\overline{G_2^2}\alpha\beta^2m^4\pi^6n^2+6\overline{l_0^2}\,\overline{G_2^2}\alpha\beta^4m^2\pi^6n^4+2\overline{l_0^2}\,\overline{G_0^2}\alpha m^4\pi^4$$
$$+2\overline{l_0^2}\,\overline{G_2^2}\alpha m^6\pi^6+\frac{12}{5}\overline{l_1^2}\,\overline{G_2^2}\alpha\beta^4m^2\pi^6n^4+\frac{16}{15}\overline{l_1^2}\,\overline{G_0^2}\alpha\beta^2m^2\pi^4n^2$$
$$+\frac{4}{5}\overline{l_1^2}\,\overline{G_2^2}\alpha\beta^6n^6\pi^6+\frac{8}{15}\overline{l_1^2}\,\overline{G_0^2}\alpha\beta^4n^4\pi^4+\frac{12}{5}\overline{l_1^2}\,\overline{G_2^2}\alpha\beta^2m^4\pi^6n^2$$
$$+\frac{8}{15}\overline{l_1^2}\,\overline{G_0^2}\alpha m^4\pi^4+\frac{4}{5}\overline{l_1^2}\,\overline{G_2^2}\alpha m^6\pi^6+3\overline{l_2^2}\,\overline{G_0^2}\alpha\beta^2m^2\pi^4n^2$$
$$+\frac{1}{2}\overline{l_2^2}\,\overline{G_0^2}\alpha m^4\pi^4+\frac{1}{2}\overline{l_2^2}\,\overline{G_0^2}\alpha\beta^4n^4\pi^4+\overline{A_{11}^2}\alpha m^4\pi^4+\overline{A_{22}^2}\alpha\beta^4n^4\pi^4$$
$$+4\overline{A_{66}^2}\alpha\beta^2m^2\pi^4n^2+2\overline{A_{12}^2}\alpha\beta^2m^2\pi^4n^2+\alpha k_1k_{w12}^*+\alpha k_{w12}^*$$
$$+\alpha\beta^2k_Gk_{Gx}^*n^2\pi^2+\alpha k_{Gx}^*m^2\pi^2, \tag{C-24}$$

$$M_{45}=-\overline{I_3^2}m\pi\ , \tag{C-25}$$

$$K_{45}=-2\overline{l_0^2}\,\overline{G_5^2}\beta^2m\pi^3n^2-2\overline{l_0^2}\,\overline{G_3^2}m^5\pi^5-2\overline{l_0^2}\,\overline{G_5^2}m^3\pi^3$$
$$-2\overline{l_0^2}\,\overline{G_3^2}\beta^4m\pi^5n^4-4\overline{l_0^2}\,\overline{G_3^2}\beta^2m^3\pi^5n^2-\frac{16}{15}\overline{l_1^2}\,\overline{G_5^2}\beta^2m\pi^3n^2$$
$$-\frac{2}{5}\overline{l_1^2}\,\overline{G_9^2}m^3\pi^3-\frac{4}{5}\overline{l_1^2}\,\overline{G_3^2}\beta^4m\pi^5n^4-\frac{4}{5}\overline{l_1^2}\,\overline{G_3^2}m^5\pi^5-\frac{16}{15}\overline{l_1^2}\,\overline{G_5^2}m^3\pi^3$$
$$-\frac{2}{5}\overline{l_1^2}\,\overline{G_7^2}\beta^2m\pi^3n^2-\frac{8}{5}\overline{l_1^2}\,\overline{G_3^2}\beta^2m^3\pi^5n^2-\frac{3}{4}\overline{l_2^2}\,\overline{G_5^2}\beta^2m\pi^3n^2$$
$$-\frac{1}{4}\overline{l_2^2}\,\overline{G_5^2}m^3\pi^3-\overline{D_{11}^2}m^3\pi^3-2\overline{D_{12}^2}\beta^2m\pi^3n^2-2\overline{D_{66}^2}\beta^2m\pi^3n^2, \tag{C-26}$$

$$M_{46}=-\overline{I_3^2}\beta n\pi\ , \tag{C-27}$$

$$K_{46}=-2\overline{l_0^2}\,\overline{G_3^2}\beta m^4\pi^5n-4\overline{l_0^2}\,\overline{G_3^2}\beta^3m^2\pi^5n^3-2\overline{l_0^2}\,\overline{G_3^2}\beta^5n^5\pi^5$$
$$-2\overline{l_0^2}\,\overline{G_5^2}\beta^3n^3\pi^3-2\overline{l_0^2}\,\overline{G_5^2}\beta m^2\pi^3n-\frac{16}{15}\overline{l_1^2}\,\overline{G_5^2}\beta^3n^3\pi^3-\frac{2}{5}\overline{l_1^2}\,\overline{G_7^2}\beta^3n^3\pi^3$$
$$-4/5\overline{l_1^2}\,\overline{G_3^2}\beta^5n^5\pi^5-\frac{4}{5}\overline{l_1^2}\,\overline{G_3^2}\beta m^4\pi^5n-\frac{16}{15}\overline{l_1^2}\,\overline{G_5^2}\beta m^2\pi^3n$$
$$-\frac{8}{5}\overline{l_1^2}\,\overline{G_3^2}\beta^3m^2\pi^5n^3-\frac{2}{5}\overline{l_1^2}\,\overline{G_9^2}\beta m^2\pi^3n-\frac{1}{4}\overline{l_2^2}\,\overline{G_5^2}\beta^3n^3\pi^3$$
$$-\frac{3}{4}\overline{l_2^2}\,\overline{G_5^2}\beta m^2\pi^3n-\overline{D_{22}^2}\beta^3n^3\pi^3-\overline{D_{12}^2}\beta m^2\pi^3n-2\overline{D_{66}^2}\beta m^2\pi^3n, \tag{C-28}$$

$$K_{47}=\frac{3}{2}\alpha h^*\overline{P_1}\pi^3m^2+\frac{3}{2}\alpha\beta^2h^*\overline{P_1}\pi^3\overline{e_{32}}n^2, \tag{C-29}$$

$$M_{54}=-\overline{I_3^2}\alpha m\pi\ , \tag{C-30}$$

$$K_{54}=-2\overline{l_0^2}\,\overline{G_5^2}\alpha m^3\pi^3-2\overline{l_0^2}\,\overline{G_3^2}\alpha m^5\pi^5-2\overline{l_0^2}\,\overline{G_3^2}\beta^4\alpha m\pi^5n^4$$
$$-2\overline{l_0^2}\,\overline{G_5^2}\beta^2\alpha m\pi^3n^2-4\overline{l_0^2}\,\overline{G_3^2}\beta^2\alpha m^3\pi^5n^2-\frac{4}{5}\overline{l_1^2}\,\overline{G_3^2}\alpha m^5\pi^5$$
$$-\frac{8}{5}\overline{l_1^2}\,\overline{G_3^2}\beta^2\alpha m^3\pi^5n^2-\frac{16}{15}\overline{l_1^2}\,\overline{G_5^2}\beta^2\alpha m\pi^3n^2-\frac{2}{5}\overline{l_1^2}\,\overline{G_7^2}\beta^2\alpha m\pi^3n^2$$
$$-\frac{4}{5}\overline{l_1^2}\,\overline{G_3^2}\beta^4\alpha m\pi^5n^4-\frac{2}{5}\overline{l_1^2}\,\overline{G_9^2}\alpha m^3\pi^3-\frac{16}{15}\overline{l_1^2}\,\overline{G_5^2}\alpha m^3\pi^3$$
$$-\frac{3}{4}\overline{l_2^2}\,\overline{G_5^2}\beta^2\alpha m\pi^3n^2-\frac{1}{4}\overline{l_2^2}\,\overline{G_5^2}\alpha m^3\pi^3-\overline{D_{11}^2}\alpha m^3\pi^3$$
$$-2\overline{D_{66}^2}\beta^2\alpha m\pi^3n^2-2\overline{D_{12}^2}\beta^2\alpha m\pi^3n^2, \tag{C-31}$$

$$M_{55}=\overline{I_4^2}, \tag{C-32}$$

$$K_{55}=2\overline{l_0^2}\,\overline{G_4^2}\beta^2m^2\pi^4n^2+2\overline{l_0^2}\,\overline{G_6^2}m^2\pi^2++2\overline{l_0^2}\,\overline{G_4^2}m^4\pi^4$$
$$+\frac{4}{5}\overline{l_1^2}\,\overline{G_7^2}m^2\pi^2+\frac{4}{5}\overline{l_1^2}\,\overline{G_4^2}m^4\pi^4+\frac{32}{15}\overline{l_1^2}\,\overline{G_6^2}m^2\pi^2+\frac{4}{3}\overline{l_1^2}\,\overline{G_4^2}\beta^2m^2\pi^4n^2$$
$$+\frac{4}{15}\overline{l_1^2}\,\overline{G_7^2}\beta^2n^2\pi^2+\frac{4}{3}\overline{l_1^2}\,\overline{G_6^2}\beta^2n^2\pi^2+\frac{8}{15}\overline{l_1^2}\,\overline{G_4^2}\beta^4n^4\pi^4+\frac{8}{15}\overline{l_1^2}\,\overline{G_8^2}$$
$$+1/8\overline{l_2^2}\,\overline{G_8^2}+\frac{1}{8}\overline{l_2^2}\,\overline{G_4^2}\beta^2m^2\pi^4n^2+\overline{l_2^2}\,\overline{G_6^2}\beta^2n^2\pi^2+\frac{1}{8}\overline{l_2^2}\,\overline{G_4^2}\beta^4n^4\pi^4$$
$$+\frac{1}{4}\overline{l_2^2}\,\overline{G_7^2}\beta^2n^2\pi^2+\frac{1}{8}\overline{l_2^2}\,\overline{G_6^2}m^2\pi^2+\overline{C_{55}^2}+\overline{B_{11}^2}m^2\pi^2+\overline{B_{66}^2}\beta^2n^2\pi^2, \tag{C-33}$$

$$K_{56}=+2\overline{l_0^2}\,\overline{G_4^2}\beta^3m\pi^4n^3+2\overline{l_0^2}\,\overline{G_4^2}\beta m^3\pi^4n+2\overline{l_0^2}\,\overline{G_6^2}\beta m\pi^2n$$
$$+\frac{4}{15}\overline{l_1^2}\,\overline{G_4^2}\beta^3m\pi^4n^3+\frac{4}{5}\overline{l_1^2}\,\overline{G_6^2}\beta m\pi^2n+\frac{4}{15}\overline{l_1^2}\,\overline{G_4^2}\beta m^3\pi^4n$$
$$+\frac{8}{15}\overline{l_1^2}\,\overline{G_7^2}\beta m\pi^2n-\frac{1}{4}\overline{l_2^2}\,\overline{G_7^2}\beta m\pi^2n-\frac{1}{8}\overline{l_2^2}\,\overline{G_4^2}\beta m^3\pi^4n$$
$$-\frac{1}{8}\overline{l_2^2}\,\overline{G_4^2}\beta^3m\pi^4n^3-\frac{5}{8}\overline{l_2^2}\,\overline{G_6^2}\beta m\pi^2n+\overline{B_{66}^2}\beta m\pi^2n+\overline{B_{12}^2}\beta m\pi^2n, \tag{C-34}$$

$$K_{57}=\frac{3}{2}\alpha\overline{P_2e_{15}}m\pi-\frac{3}{2}\alpha h^*\overline{P_5}\pi^2m, \tag{C-35}$$

$$M_{64}=-\overline{I_3^2}\alpha\beta n\pi, \tag{C-36}$$

$$K_{64}=-2\overline{l_0^2}\,\overline{G_5^2}\alpha\beta m^2\pi^3n-2\overline{l_0^2}\,\overline{G_3^2}\alpha\beta^5n^5\pi^5-2\overline{l_0^2}\,\overline{G_5^2}\alpha\beta^3n^3\pi^3$$
$$-2\overline{l_0^2}\,\overline{G_3^2}\alpha\beta m^4\pi^5n-4\overline{l_0^2}\,\overline{G_3^2}\alpha\beta^3m^2\pi^5n^3-\frac{2}{5}\overline{l_1^2}\,\overline{G_7^2}\alpha\beta^3n^3\pi^3$$
$$-\frac{2}{5}\overline{l_1^2}\,\overline{G_9^2}\alpha\beta m^2\pi^3n-\frac{4}{5}\overline{l_1^2}\,\overline{G_3^2}\alpha\beta^5n^5\pi^5-\frac{16}{15}\overline{l_1^2}\,\overline{G_5^2}\alpha\beta m^2\pi^3n$$
$$-\frac{8}{5}\overline{l_1^2}\,\overline{G_3^2}\alpha\beta^3m^2\pi^5n^3-\frac{16}{15}\overline{l_1^2}\,\overline{G_5^2}\alpha\beta^3n^3\pi^3-\frac{4}{5}\overline{l_1^2}\,\overline{G_3^2}\alpha\beta m^4\pi^5n$$
$$-\frac{3}{4}\overline{l_2^2}\,\overline{G_5^2}\alpha\beta m^2\pi^3n-\frac{1}{4}\overline{l_2^2}\,\overline{G_5^2}\alpha\beta^3n^3\pi^3-\overline{D_{22}^2}\alpha\beta^3n^3\pi^3$$
$$-2\overline{D_{66}^2}\alpha\beta m^2\pi^3n-\overline{D_{12}^2}\alpha\beta m^2\pi^3n, \tag{C-37}$$

$$K_{65}=2\overline{l_0^2}\,\overline{G_6^2}\beta m\pi^2n+2\overline{l_0^2}\,\overline{G_4^2}\beta^3m\pi^4n^3+2\overline{l_0^2}\,\overline{G_4^2}\beta m^3\pi^4n$$
$$+4/5\overline{l_1^2}\,\overline{G_6^2}\beta m\pi^2n+\frac{4}{15}\overline{l_1^2}\,\overline{G_4^2}\alpha\beta^3m\pi^4n^3+\frac{8}{15}\overline{l_1^2}\,\overline{G_7^2}\beta m\pi^2n$$
$$+\frac{4}{15}\overline{l_1^2}\,\overline{G_4^2}\beta m^3\pi^4n-\frac{1}{4}\overline{l_2^2}\,\overline{G_7^2}\beta m\pi^2n-\frac{5}{8}\overline{l_2^2}\,\overline{G_6^2}\beta m\pi^2n$$
$$-\frac{1}{8}\overline{l_2^2}\,\overline{G_4^2}\beta^3m\pi^4n^3-\frac{1}{8}\overline{l_2^2}\,\overline{G_4^2}\beta m^3\pi^4n+\overline{B_{66}^2}\beta m\pi^2n+\overline{B_{12}^2}\beta m\pi^2n, \tag{C-38}$$

$$M_{66}=\overline{I_4^2}, \tag{C-39}$$

$$
\begin{aligned}
K_{66} =& 2\overline{l_0}^2\overline{G_6^2}\beta^2n^2\pi^2 + 2\overline{l_0}^2\overline{G_4^2}\beta^4n^4\pi^4 + 2\overline{l_0}^2\overline{G_4^2}\beta^2m^2\pi^4n^2 \\
&+\frac{4}{5}\overline{l_1}^2\overline{G_7^2}\beta^2n^2\pi^2 + \frac{4}{5}\overline{l_1}^2\overline{G_4^2}\beta^4n^4\pi^4 + \frac{32}{15}\overline{l_1}^2\overline{G_6^2}\beta^2n^2\pi^2 + \frac{8}{15}\overline{l_1}^2\overline{G_8^2} \\
&+\frac{4}{15}\overline{l_1}^2\overline{G_7^2}m^2\pi^2 + \frac{4}{3}\overline{l_1}^2\overline{G_4^2}\beta^2m^2\pi^4n^2 + \frac{4}{3}\overline{l_1}^2\overline{G_6^2}m^2\pi^2 \\
&+\frac{8}{15}\overline{l_1}^2\overline{G_4^2}m^4\pi^4 + \frac{1}{8}\overline{l_2}^2\overline{G_8^2} + \frac{1}{4}\overline{l_2}^2\overline{G_7^2}m^2\pi^2 + \frac{1}{8}\overline{l_2}^2\overline{G_4^2}m^4\pi^4 \\
&+\frac{1}{8}\overline{l_2}^2\overline{G_6^2}\beta^2n^2\pi^2 + \overline{l_2}^2\overline{G_6^2}m^2\pi^2 + \frac{1}{8}\overline{l_2}^2\overline{G_4^2}\beta^2m^2\pi^4n^2 \\
&+\overline{B_{22}^2}\beta^2n^2\pi^2 + \overline{B_{66}^2}m^2\pi^2 + \overline{C_{44}^2},
\end{aligned}
\tag{C-40}
$$

$$
K_{67} = \frac{3}{2}\alpha\beta\overline{P_2}\overline{e_{24}}n\pi - \frac{3}{2}\alpha\beta h^*\overline{P_5}\overline{e_{32}}\pi^2n, \tag{C-41}
$$

$$
K_{74} = \frac{3}{2}\alpha^2h^*\overline{P_1}\pi^3m^2 + \frac{3}{2}\alpha^2\beta^2h^*\overline{P_1}\overline{e_{32}}\pi^3n^2, \tag{C-42}
$$

$$
K_{75} = \frac{3}{2}\alpha\overline{P_2}\overline{e_{15}}m\pi - \frac{3}{2}\alpha h^*\overline{P_5}\pi^2m, \tag{C-43}
$$

$$
K_{76} = \frac{3}{2}\alpha\beta\overline{P_2}\overline{e_{24}}n\pi - \frac{3}{2}\alpha\beta h^*\overline{P_5}\overline{e_{32}}\pi^2n, \tag{C-44}
$$

$$
K_{77} = -2\alpha\overline{P_4}\overline{\in_{11}}m^2\pi^2 - 2\alpha\beta^2\overline{P_4}\overline{\in_{22}}n^2\pi^2 - 2\frac{h^{*2}\overline{P_3}\overline{\in_{33}}\pi^2}{\alpha}, \tag{C-45}
$$

Note that the coefficients of Matrices *M*, *C* and *K* where aren't mentioned, are equal to zero.